A New Method to Calculate Transition Lines near the Multicritical Point using Twisted Boundary Conditions

守屋, 俊志

A New Method to Calculate Transition Lines near the Multicritical Point using Twisted Boundary Conditions

Shunji Moriya

February 22, 2022

Abstract

A point where several critical lines intersect is called a multicritical point. Near such a point, multiple critical phenomena interfere and a finite-size correction becomes large. Therefore, conventional methods cannot be applied near the multicritical point. We propose a new method to numerically calculate a transition point for a quantum spin chain near the multicritical point.

We treat a bond-alternating (BA) XXZ model for $S = 1/2, 1, 3/2$. In a ground-state phase diagram of this model, a 2D Gaussian universality transition line bifurcates into two 2D Ising universality transition lines, which make a multicritical point. At this point, Berezinskii-Kosterlitz-Thouless transition occurs, where the correlation length diverges singularly.

To deal with a 2D Ising universality, we review a transverse field 1D quantum Ising (TFI) model, corresponding to the classical 2D Ising model with transfer matrix. A relation between a disorder phase and an order phase is known as the Kramers-Wannier duality transformation. We find a proper duality transformation that is exact in the finite-size TFI model with a periodic and anti-periodic boundary condition. This shows that the energies for the two boundary conditions are crossing at the transition point. A free fermion field theory is derived from the critical Ising model by taking a continuum limit. From a conformal field theory, we verify that the energy-crossing is realized in the 2D Ising universality class, not only in the TFI model.

We apply our method to the BA XXZ model. The energy-crossing happens in boundary conditions that are twisted around a z-axis and y-axis. In an anisotropic limit, two energies in a finite-size are crossing at the transition point since the BA XXZ model is identical to the TFI model. on the other hand, at the multicritical point, the finite-size correction vanishes by an isotropy and a twist translation symmetry. Therefore, near the multicritical point, our method has a smaller finite-size correction.

In this paper, we also review the 2D Gaussian universality. By a bosonization, the BA XXZ model can be transformed to a phase Hamiltonian composed of boson operators. The degenerate energies for a twisted boundary condition are split by a perturbation around a Gaussian fixed point.

By our method, we numerically calculate a transition point of the BA XXZ model for $S = 1/2, 1, 3/2$. As expected, the finite-size correction of numerical results becomes very small near the multicritical point.

Contents

Chapter 1

Introduction

1.1 Critical Phenomena

Critical phenomena are interesting subjects in condensed matter physics. To understand the critical phenomena, it is important to find a transition point. For unsolvable models, a numerical calculation is an important way to determine where it occurs. Although critical phenomena occur only in infinite systems, the number of particle or spin is limited by numerical resources. Therefore, sometimes we cannot obtain reliable results due to a finite-size correction (FSC). Moreover, since various critical phenomena interfere near a multicritical point, the FSC becomes larger. One example for a multicritical point is shown in Fig.1.1. In previous researches, several methods to calculate a transition point have been proposed[1][2]. However, these conventional methods can not calculate a reliable transition point near a multicritical point.

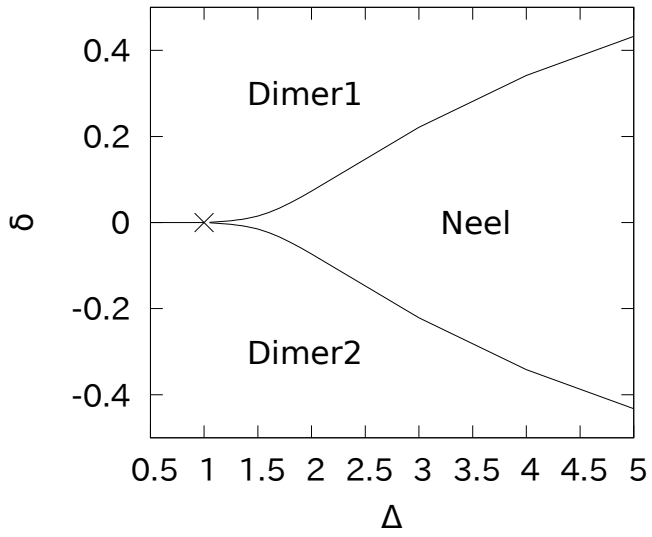

Figure 1.1: The phase diagram of the BA XXZ model. The multicritical point is denoted by $\times$. Two transition lines get closer near the multicritical point.

1.2 Bond-Alternating XXZ chain

As a model that has a multicritical point, we treat a bond-alternating (BA) XXZ chain in this thesis.

1.2.1 Hamiltonian

The Hamiltonian of the BA XXZ chain is

$$\hat{H}(\delta,\Delta)=\sum_{j}^{N}\left[1-(-1)^{j}\delta\right]\left(\hat{S}_{j}^{x}\hat{S}_{j+1}^{x}+\hat{S}_{j}^{y}\hat{S}_{j+1}^{y}+\Delta\hat{S}_{j}^{z}\hat{S}_{j+1}^{z}\right), \tag{1.2.1}$$

$\hat{S}_j^i$'s are the spin operators ($i=x,y,z$). The commutation relations are

$$\left[\hat{S}_{j}^{k},\hat{S}_{j'}^{l}\right]=i\delta_{jj'}\sum_{m=1}^{3}\epsilon_{klm}\hat{S}_{j}^{m}. \tag{1.2.2}$$

The $[1-(-1)^j\delta]$ is the bond-alternation coefficient. For $\delta>0$, a bond between $2j$ and $2j+1$ takes a stronger interaction than $2j-1$ and $2j$ bond. The Δ makes anisotropy in the z-direction. We take the system size even, $N=2n$ (n is an integer). The Ashkin-Teller model is known as an equivalent model of BA XXZ chain [3, 4, 5] (Appendix A).

1.2.2 Symmetry

The BA XXZ model has the following symmetries and conserved quantities.

- The Hamiltonian is invariant for a spin θ-rotation of all-sites around the z-axis

$$\hat{U}_\theta^z = \exp\left(i\theta \sum_j \left(\hat{S}_j^z - \frac{1}{2}\right)\right). \tag{1.2.3}$$

  The conserved quantity is a magnetization

$$M = \sum_j S_j^z. \tag{1.2.4}$$

- Because of the anisotropy, the Hamiltonian is invariant for a spin π-rotation around the y-axis,

$$\hat{U}_\pi^y = \exp\left(i\pi \sum_j \left(\hat{S}_j^y - \frac{1}{2}\right)\right). \tag{1.2.5}$$

  The conserved quantity is a parity of a spin reversal

$$U_\pi^y = \pm 1. \tag{1.2.6}$$

- We define the translational operator $\hat{T}_R$,

$$\hat{T}_R \hat{\boldsymbol{S}}_j \hat{T}_R^{-1} = \hat{\boldsymbol{S}}_{j+1}. \tag{1.2.7}$$

  For $\delta \neq 0$, the Hamiltonian has a two-site translational symmetry,

$$(\hat{T}_R)^2 \hat{H} (\hat{T}_R)^{-2} = \hat{H}, \tag{1.2.8}$$

  in the periodic boundary condition (PBC)

$$\hat{\boldsymbol{S}}_{L+1}^x = \hat{\boldsymbol{S}}_1^x. \tag{1.2.9}$$

  Since the N-site translation is an identity operator,

$$(\hat{T}_R)^N = \hat{1}, \tag{1.2.10}$$

  the eigenvalue of $\hat{T}_R$ is

$$T_R = \exp iq, \quad (q = 0, \frac{2\pi}{N}, \cdots, \frac{2\pi(N-1)}{N}). \tag{1.2.11}$$

The change of the sign of the bond-alternation parameter δ is regarded as one-site translation,

$$\hat{T}_R \hat{H}(-\delta, \Delta) \hat{T}_R^{-1} = \hat{H}(\delta, \Delta), \tag{1.2.12}$$

and therefore, the model has the same energy-spectrum for the opposite sign.

1.2.3 Solvable Region for S=1/2

- $\delta = \pm 1, \Delta > 0$
  The model is reduced to a sum of isolated two spins. The ground-state is a direct product of singlet pairs

$$(|\uparrow\rangle|\downarrow\rangle - |\downarrow\rangle|\uparrow\rangle)(|\uparrow\rangle|\downarrow\rangle - |\downarrow\rangle|\uparrow\rangle)\cdots . \tag{1.2.13}$$

  The spin reversal symmetry $U_\pi^y = (-1)^{N/2}$ is not broken.

- $\Delta \to \infty$
  The z-direction is dominant. The ground-state is doubly degenerate Néel state,

$$|\uparrow\downarrow\uparrow\downarrow\uparrow\downarrow\cdots\rangle \quad \text{and} \quad |\downarrow\uparrow\downarrow\uparrow\downarrow\uparrow\cdots\rangle . \tag{1.2.14}$$

  The spin reversal symmetry is broken.

- $\delta = 0$ for S=1/2
  The Bethe ansatz [6] gives an exact solution for the S=1/2 XXZ chain. At the isotropic point, $\Delta = 1$, a Berezinskii-Kosterlitz-Thouless (BKT) transition occurs, where the correlation length diverges singularly, $\xi \sim \exp\left(\frac{C}{\sqrt{\Delta - 1}}\right)$ [7]. (C is a constant.)

1.2.4 Phase Transition

In the intermediate region, $0 < \Delta < \infty, 0 < \delta < 1$, phase transitions may occur. The phase diagram is Fig.1.1. The bond-alternation makes the spins to take the singlet pairing, called a dimer phase. The ground-state is unique and has an energy gap. By the anisotropy $\Delta > 1$, the neighbouring spins tend to take the opposite direction, called a Néel phase. There are doubly degenerate ground-state and spontaneous breaking of the spin reversal symmetry. The phase transition between the dimer and the Néel phase belongs to a 2D Ising universality class.

There are two types of dimer phase. In $\delta > 0$, spins on the $2j$ and $2j+1$ site form a singlet, called a dimer1 phase. On the contrary, in $\delta < 0$, the singlet pair is formed on the $2j-1$ and $2j$ site, a dimer2 phase. The 2D Gaussian transition occurs in a boundary between the dimer1 and the dimer2 phase. For S=1/2, this transition line is exactly $\delta = 0$, verified from a symmetry with a twisted boundary condition[8].

The 2D Gaussian transition line bifurcates into two 2D Ising transition lines, that makes a multicritical point. This point is called an Ashkin-Teller multicritical point (from now on, we abbreviate it as an AT point). The 2D Ising transition lines get closer near the multicritical point. Thereby, the correlation length becomes large, which brings a difficulty in a finite-size numerical calculation.

1.3 Haldane conjecture

The BA XXZ model has a different characteristic depending on the value of S. For the case of $\Delta = 1, \delta = 0$, a Heisenberg model, Haldane[9] predicted about an energy gap as follows. A half-odd integer spin chain has a degenerate ground state, which is gapless. On the other hand, the integer spin chain has a unique disordered ground state, which has an energy gap. The XXZ chain for $S = 1/2$ is exactly solvable by Bethe ansatz and known as gapless at the isotropic point, which agree with the Haldane conjecture. The solvability is broken by an addition of another interaction term, for example, the bond-alternation. In general, the XXZ chain for $S > 1/2$ is unsolvable.

1.4 Level Spectroscopy Method

A useful method to calculate a transition point, a *Level Spectroscopy* (LS) method was proposed by Nomura. The LS method cancels logarithmic corrections of a Berezinskii-Kosterlitz-Thouless (BKT) transition by using the z-axis twisted boundary condition [10, 11, 12]. Some universality class can be calculated by the LS method, for example a 2D Gaussian one, Sec 3.3. However, we can not calculate 2D Ising universality transition by the LS method. So, we propose a new method applicable to a 2D Ising universality.

1.5 Organization of this thesis

This thesis is organized as follows. In Chap. 2, we deal with a 2D Ising universality. We review a correspondence between a 2D classical Ising and a 1D quantum Ising model. By the Kramers-Wannier duality, energy-crossings are proved. In addition, we review an exact solution by Lieb *et al*[15].

For a continuum limit, we verify that the energy-crossing is realized in a 2D Ising universality class (Sec 2.3) by a free fermion conformal field theory. Our new method is proposed in Sec 2.4.3. The finite-size correction is discussed in Sec 2.4.4. Next, we deal with a 2D Gaussian universality in Chap. 3. By bosonization, the bond-alternating XXZ chain is converted to a phase Hamiltonian, Sec 3.2. The perturbative calculation around a fixed point is described in Sec 3.3. The numerical results for $S = 1/2, 1, 3/2$ are shown in Chap. 4.

Chapter 2

2D Ising Universality Class

In this chapter, we review properties of an Ising model. By using a transfer matrix, a quantum 1D Ising model is derived from a classical 2D Ising model. This quantum model has the Kramers-Wannier duality, that relates an order phase to a disorder phase. By this duality, for a finite system, energies for different boundary conditions cross at a critical point. To consider a continuum limit, we discuss a conformal field theory of a free fermion.

Finally, we introduce a method to calculate a 2D Ising universality transition point. The smallness of the FSC is also explained.

2.1 2D classical Ising model

The 2D classical Ising model on a square lattice (Fig.2.1) is defined as

$$H = -\left(J_1 \sum_{i,j}^{M,N} \sigma_{i,j}\sigma_{i+1,j} + J_2 \sum_{i,j}^{M,N} \sigma_{i,j}\sigma_{i,j+1} \right). \tag{2.1.1}$$

Each classical Ising spin σ takes two possible values $\sigma_{i,j} = \pm 1$. The spins interact with nearest neighbor spins. This model was solved firstly by Onsager[13]. The transition temperature T_c satisfies $\sinh(2J_1/k_{\mathrm{B}}T_c)\sinh(2J_2/k_{\mathrm{B}}T_c) = 1$.

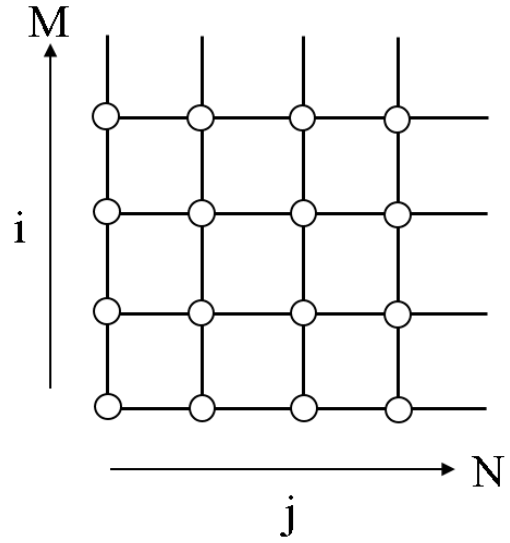

Figure 2.1: The 2D $M \times N$ square lattice. Each spin is localized on $\circ$.

2.1.1 Classical-Quantum Correspondence

We review a correspondence between the classical 2D and the quantum 1D Ising model using the transfer matrix [14][15]. The partition function for the 2D classical Ising model is calculated as

$$\begin{aligned} Z &= \sum_{\sigma=\pm 1} \exp\left(-\beta H\right) \\ &= \sum_{\sigma=\pm 1} \exp\left(K_1 \sum_{i,j}^{M,N} \sigma_{i,j}\sigma_{i+1,j} + K_2 \sum_{i,j}^{M,N} \sigma_{i,j}\sigma_{i,j+1} \right), \end{aligned} \tag{2.1.2}$$

where $K_1 = \beta J_1, K_2 = \beta J_2$. The summation is taken over all spin-configurations

$$\sum_{\sigma=\pm 1} \equiv \sum_{\sigma_1=\pm 1} \sum_{\sigma_2=\pm 1} \sum_{\sigma_3=\pm 1} \cdots \sum_{\sigma_N=\pm 1} . \tag{2.1.3}$$

We rewrite the summation for j as a product sum

$$Z = \sum_{\sigma=\pm 1} \prod_{j}^{N} \exp\left(K_1 \sum_{i}^{M} \sigma_{i,j}\sigma_{i+1,j} + K_2 \sum_{i}^{M} \sigma_{i,j}\sigma_{i,j+1} \right). \tag{2.1.4}$$

Firstly, we deal with the case where spins interact only in the i-direction, in other words, $K_2 = 0$. The summation can be calculated using the 2×2 matrices

$$\begin{aligned} (v_j)_{\sigma_{i,j}\sigma_{i+1,j}} &= \exp\left(K_1 \sigma_{i,j}, \sigma_{i+1,j}\right) \\ v_j &= \begin{pmatrix} \mathrm{e}^{K_1} & \mathrm{e}^{-K_1} \\ \mathrm{e}^{-K_1} & \mathrm{e}^{K_1} \end{pmatrix} \end{aligned} \tag{2.1.5}$$

The partition function is calculated by the trace of a matrix product.

$$Z = \mathrm{Tr}\,(v_1 \otimes \cdots \otimes v_N)^M \tag{2.1.6}$$

Using the Pauli matrix, each v_j is represented as

$$v_j = \mathrm{e}^{K_1}\hat{I}_j + \mathrm{e}^{-K_1}\hat{\tau}_j^x. \tag{2.1.7}$$

The $\hat{I}_j$ is an identity operator. The Pauli matrices are

$$\hat{\tau}_j^x = \begin{pmatrix} 0 & 1 \\ 1 & 0 \end{pmatrix}, \hat{\tau}_j^y = \begin{pmatrix} 0 & -i \\ i & 0 \end{pmatrix}, \hat{\tau}_j^z = \begin{pmatrix} 1 & 0 \\ 0 & -1 \end{pmatrix}, \tag{2.1.8}$$

which satisfy the commutation relations

$$\left[\hat{\tau}_j^k, \hat{\tau}_{j'}^l\right] = 2i\delta_{jj'}\sum_{m=1}^{3}\epsilon_{klm}\hat{\tau}_j^m, \tag{2.1.9}$$

$$\left\{\hat{\tau}_j^k, \hat{\tau}_j^l\right\} = 2\delta_{kl}\hat{I}. \tag{2.1.10}$$

Here, we denote the Pauli matrix by $\hat{\tau}_i^j$ to avoid the confusion with the classical variables σ already introduced. Because $\left(\hat{\tau}_i^j\right)^2 = \hat{I}$, the following equation is satisfied :

$$\exp\left(a\hat{\tau}^i\right) = \cosh a\left(\hat{I} + \hat{\tau}^i \tanh a\right), \tag{2.1.11}$$

which is easily checked by performing the Taylor expansion. Then the transfer matrix v_j is written as an exponential function of Pauli operator,

$$v_j = (2\sinh 2K_1)^{1/2}\exp\left(K_1^*\hat{\tau}_j^x\right), \tag{2.1.12}$$

where K_1^* is defined by

$$\tanh K_1^* \equiv \mathrm{e}^{-2K_1}. \tag{2.1.13}$$

Summing over j, we obtain

$$\begin{aligned} V \equiv & v_1 \otimes \cdots \otimes v_N \\ = & (2\sinh 2K_1)^{N/2}\exp\left(K_1^*\sum_j^N \hat{\tau}_j^x\right) \end{aligned} \tag{2.1.14}$$

Next, we consider the second term in thethe Hamiltonian Eq.(2.1.1). Before treating the interaction between two spins, we deal with the case where an external field exists, $H_h = h\sum \sigma_{i,j}$, The transfer matrix for H_h is

$$\begin{aligned} w_j' = & \begin{pmatrix} \mathrm{e}^h & 0 \\ 0 & \mathrm{e}^{-h} \end{pmatrix} \\ = & \exp\left(h\hat{\tau}_j^z\right). \end{aligned} \tag{2.1.15}$$

Then the transfer matrix for the interaction term ($K_2 \sum \sigma_{i,j}\sigma_{i,j+1}$) becomes

$$w_j = \exp\left(K_2 \hat{\tau}_j^z \hat{\tau}_{j+1}^z\right) \tag{2.1.16}$$

Summing over j, we obtain

$$W \equiv \prod_N^j w_j = \exp\left(K_2 \sum_j^N \hat{\tau}_j^z \hat{\tau}_{j+1}^z\right). \tag{2.1.17}$$

We arrive at the transfer matrix form of the partition function

$$Z = \mathrm{Tr}\,(VW)^M \tag{2.1.18}$$

$$= (2\sinh 2K_1)^{N/2} \exp\left(K_1^* \sum_j^N \hat{\tau}_j^x\right) \exp\left(K_2 \sum_j^N \hat{\tau}_j^z \hat{\tau}_{j+1}^z\right). \tag{2.1.19}$$

We try to bring the two sum in the exponent of V and W into one exponent. We use the Campbell-Baker-Hausdorff formula

$$\exp(A)\exp(B) = \exp\left(A + B + \frac{1}{2}[A,B] + \frac{1}{12}[A-B,[A,B]] + \cdots\right). \tag{2.1.20}$$

In this case, the two operators do not commute, that is ,

$$\left[K_1^* \sum_j^N \hat{\tau}_j^x, K_2 \sum_j^N \hat{\tau}_j^z \hat{\tau}_{j+1}^z\right] \neq 0. \tag{2.1.21}$$

If taking the limit

$$K_1^* K_2 \to 0, \tag{2.1.22}$$

we obtain the quantum-classical correspondence

$$V_1 V_2 = (2\sinh 2K_1)^{N/2} \exp\left(K_1^* \sum_j^N \hat{\tau}_j^x + K_2 \sum_j^N \hat{\tau}_j^z \hat{\tau}_{j+1}^z.\right). \tag{2.1.23}$$

To maintain the dimensionality, we need a constraint for the ratio

$$\gamma \equiv \frac{K_1^*}{K_2} = \text{finite}. \tag{2.1.24}$$

In 2D classical Ising language, this limit corresponds to the anisotropy limit in directions of interaction

$$K_1 \to \infty, K_2 \to 0, \tag{2.1.25}$$

which can be easily calculated from Eq.(2.1.13).

2.2 Transverse Field Ising model

We obtain a transverse Field quantum Ising (TFI) model Eq.(2.1.23),

$$\hat{H} = -\frac{\gamma}{2}\sum_{j=1}^{N}\hat{\sigma}_j^x - \sum_{j=1}^{N-1}\hat{\sigma}_j^z\hat{\sigma}_{j+1}^z + g\hat{\sigma}_N^z\hat{\sigma}_1^z. \tag{2.2.1}$$

The $\hat{\sigma}_j^i$'s are the Pauli matrices ($i = x, y, z$). Settling $g = 1$ (-1) corresponds to imposing a periodic (an anti-periodic) BC. This model has a translational ($\hat{\boldsymbol{\sigma}}_j \to \hat{\boldsymbol{\sigma}}_{j+1}$) symmetry for $g = 1$ and spin reversal ($\hat{\sigma}^z \to -\hat{\sigma}^z$) symmetry. If the transverse field is dominant ($\gamma \to \infty$), there is no interaction, and a unique ground state is a disordered state

$$\left(|\uparrow\rangle + |\downarrow\rangle\right)\left(|\uparrow\rangle + |\downarrow\rangle\right)\cdots.$$

The spin reversal symmetry is $U_\pi^x = (-1)^N$. If there is no transverse field ($\gamma = 0$), ground states are doubly degenerate

$$|\uparrow\uparrow\uparrow\uparrow\cdots\rangle, \quad |\downarrow\downarrow\downarrow\downarrow\cdots\rangle,$$

which break the spin reversal symmetry. The phase transition occurs in an intermediate region ($0 < \gamma < \infty$). We derive the transition point, using a duality.

2.2.1 Duality

The Ising model has the Kramers-Wannier duality [16], that relates a order phase to a disorder phase. The conventional duality transformation [17] for the TFI model is only valid in a bulk. But, at a boundary, the extra terms appear, which make it impossible to demonstrate a duality for a finite system. Evans and Levis [18] introduced a duality transformation for fermion operators. Utilizing this, we improve the duality for spin operators, which enable one to treat boundary conditions and symmetry of eigenstates for a finite system. We define the duality transformation for $\hat{\sigma}_j^z$

$$\hat{\sigma}_j^z = i\hat{\tau}_1^z\prod_{k=1}^{j}\hat{\tau}_k^x. \tag{2.2.2}$$

The $\hat{\boldsymbol{\tau}}$ is a Pauli operator. In the bulk, for $1 \le j < N$, we obtain

$$\hat{\sigma}_j^z\hat{\sigma}_{j+1}^z = \hat{\tau}_{j+1}^x, \tag{2.2.3}$$

but at the boundary, $j = N$,

$$\begin{aligned}\hat{\sigma}_N^z\hat{\sigma}_1^z =& \left(\prod_{1\le j\le N}\hat{\tau}_j^x\right)\hat{\tau}_1^x \\ =& \hat{\tau}_1^x U_\pi^x(\tau).\end{aligned} \tag{2.2.4}$$

Here, $U_\pi^x(\tau)$ is a π-rotation operator about x-axis for all τ spin operator, in other word, a spin reversal operator.

The duality transformation for $\hat{\sigma}_j^x$ for $1 \leq j < N$ is

$$\hat{\sigma}_j^x = \hat{\tau}_j^z \hat{\tau}_{j+1}^z, \tag{2.2.5}$$

and for $j = N$,

$$\hat{\sigma}_N^x = \hat{\tau}_N^z \hat{\tau}_1^z U_\pi^x(\tau). \tag{2.2.6}$$

The operator $\hat{\boldsymbol{\tau}}$ satisfies the commutation relation of Pauli operators, Eqs.(2.1.9) and (2.1.10). The Hamiltonian becomes

$$\hat{H} = \gamma \left(-\sum_{j=1}^{N-1} \hat{\tau}_j^z \hat{\tau}_{j+1}^z - \hat{\tau}_N^z \hat{\tau}_1^z U_\pi^x(\tau) - \sum_{j=2}^{N} \frac{1}{\gamma} \hat{\tau}_j^x - g \frac{1}{\gamma} \hat{\tau}_1^x U_\pi^x(\tau) \right). \tag{2.2.7}$$

From Eq.(2.2.5) and Eq.(2.2.6) , we notice that

$$\begin{aligned} U_\pi^x(\sigma) =& \prod_{j=1}^{N} \hat{\sigma}_j^x, \\ =& \left(\prod_{j=1}^{N-1} \hat{\tau}_j^z \hat{\tau}_{j+1}^z \right) \hat{\tau}_N^z \hat{\tau}_1^z U_\pi^x(\tau), \\ =& U_\pi^x(\tau), \end{aligned} \tag{2.2.8}$$

and thus the spin reversal symmetry is unchanged after duality transformation. For example, we describe the case of $N = 2n$ $(n = 1, 2, \cdots)$, $g = 1$.

- In the subspace of $U_\pi^x(\sigma) = 1$,
  After the duality transformation, the Hamiltonian becomes periodic BC ($\hat{\tau}_{N+1}^z = \hat{\tau}_1^z$),

  $$\hat{H} = \gamma \left(-\sum_{j=1}^{N-1} \hat{\tau}_j^z \hat{\tau}_{j+1}^z - \hat{\tau}_N^z \hat{\tau}_1^z - \sum_{j=2}^{N} \frac{1}{\gamma} \hat{\tau}_j^x - \frac{1}{\gamma} \hat{\tau}_1^x \right). \tag{2.2.9}$$

  Then, the eigenvalue for σ and τ are related as

  $$E(g = 1, U_\pi^x = 1, \gamma) = \gamma E(g = 1, U_\pi^x = 1, 1/\gamma). \tag{2.2.10}$$

  This equation corresponds to a relation between high temperature and low temperature phase in the classical 2D Ising model. Assuming the uniqueness of the phase transition point, it occurs at a self-dual point ($\gamma = 1$), that agrees with the exact solution by Onsager [13].

- In the subspace of $U_\pi^x(\sigma) = -1$,
  we obtain the following Hamiltonian,

$$\hat{H} = \gamma \left(-\sum_{j=1}^{N-1} \hat{\tau}_j^z \hat{\tau}_{j+1}^z + \hat{\tau}_N^z \hat{\tau}_1^z - \sum_{j=2}^{N} \frac{1}{\gamma} \hat{\tau}_j^x + \frac{1}{\gamma} \hat{\tau}_1^x \right). \tag{2.2.11}$$

  By operating π-rotation for the 1st spin about the z-axis, $\hat{u}^z \equiv_\pi \exp\left(i\frac{\pi}{2}(\hat{\tau}_1^z - 1)\right)$, we obtain the TFI Hamiltonian with an anti-periodic BC ($\hat{\tau}_{N+1}^z = -\hat{\tau}_1^z$)

$$\hat{u}_1^z \hat{H} (\hat{u}_1^z)^{-1} = \gamma \left(-\sum_{j=1}^{N-1} \hat{\tau}_j^z \hat{\tau}_{j+1}^z + \hat{\tau}_N^z \hat{\tau}_1^z - \sum_{j=2}^{N} \frac{1}{\gamma} \hat{\tau}_j^x - \frac{1}{\gamma} \hat{\tau}_1^x \right). \tag{2.2.12}$$

  The $\hat{u}_1^z$ anti-commutates with the spin reversal operator,

$$\hat{U}_\pi^x \hat{u}_1^z = -\hat{u}_1^z \hat{U}_\pi^x. \tag{2.2.13}$$

  By operating to the eigenstate of the Hamiltonian, Eq.(2.2.11),

$$\begin{aligned} \hat{U}_\pi^x \hat{u}_1^z |U_\pi^x = -1\rangle =& -\hat{u}_1^z \hat{U}_\pi^x |U_\pi^x = -1\rangle \\ =& \hat{u}_1^z |U_\pi^x = -1\rangle . \end{aligned} \tag{2.2.14}$$

  the $\exp(i\pi\hat{\tau}_1^z)$ changes the spin reversal symmetry,

$$\hat{u}_1^z |U_\pi^x = -1\rangle = |U_\pi^x = 1\rangle . \tag{2.2.15}$$

We do not write the detailed calculations for the other cases, but summarize the results in Table.2.1.

For $\hat{\boldsymbol{\sigma}}$	For $\hat{\boldsymbol{\tau}}$
$U_\pi^x = 1$ Periodic	$U_\pi^x = 1$ Periodic
$U_\pi^x = -1$ Periodic	$U_\pi^x = 1$ Anti-periodic
$U_\pi^x = 1$ Anti-periodic	$U_\pi^x = -1$ Periodic
$U_\pi^x = -1$ Anti-periodic	$U_\pi^x = -1$ Anti-periodic

Table 2.1: The duality for different BC's.

The 2nd and 3rd rows of Table.2.1 show that the energies of $U_\pi^x = -1$ for periodic BC and of $U_\pi^x = 1$ for anti-periodic BC cross at the transition point.

2.2.2 Exact solution

We can also verify the energy crossing ,Eq.(2.2.10), from the exact solution of the TFI model. We review shortly the exact solution for periodic [14][15] and anti-periodic

BCs [19]. We perform the Jordan-Wigner transformation and the Fourier transformation for the Pauli operators. For convenience, we rotate all spin by $\pi/2$ around y-axis, and the Hamiltonian reads

$$\begin{aligned}\hat{H} =& -\gamma \sum_j^N \hat{\sigma}_j^z - \sum_j^N \hat{\sigma}_j^x \hat{\sigma}_{j+1}^x, \\ =& -\gamma \sum_j^N \hat{\sigma}_j^z - \sum_j^N \left(\hat{\sigma}_j^+ + \hat{\sigma}_j^-\right)\left(\hat{\sigma}_{j+1}^+ + \hat{\sigma}_{j+1}^-\right). \end{aligned} \tag{2.2.16}$$

Here, we introduce the ladder operators, $\hat{\sigma}_\pm = \hat{\sigma}^x \pm i\hat{\sigma}^y$. The Jordan-Wigner transformation is

$$\hat{\sigma}_j^+ = \exp\left(i\pi \sum_{l=1}^{j-1} \hat{a}_l^\dagger \hat{a}_l\right)\hat{a}_j^\dagger, \tag{2.2.17}$$

$$\hat{\sigma}_j^z = -1 + 2\hat{a}_j^\dagger \hat{a}_j, \tag{2.2.18}$$

where $\hat{a}_j, \hat{a}_j^\dagger$ are fermion creation and anti-creation operators. In the bulk,

$$\hat{\sigma}_j^+ \hat{\sigma}_{j+1}^- = \hat{a}_j^\dagger \hat{a}_{j+1}, \tag{2.2.19}$$

$$\hat{\sigma}_j^+ \hat{\sigma}_{j+1}^+ = \hat{a}_j^\dagger \hat{a}_{j+1}^\dagger, \tag{2.2.20}$$

but at the boundary,

$$\hat{\sigma}_N^+ \hat{\sigma}_1^- = -(-1)^{\hat{\mathcal{M}}} \hat{a}_N^\dagger \hat{a}_1, \tag{2.2.21}$$

($\hat{\mathcal{M}} = \sum_j^N \hat{a}_j^\dagger \hat{a}_j$). Performing the Fourier transformation

$$\hat{a}_j = \frac{1}{\sqrt{N}} \sum_k \mathrm{e}^{ikn} \hat{a}_k, \tag{2.2.22}$$

the Hamiltonian becomes

$$\hat{H} = \sum^k \left(\hat{a}_k^\dagger - \hat{a}_k\right)\left(\hat{a}_{k+1}^\dagger + \hat{a}_{k+1}\right) + \gamma \sum^k \left(\hat{a}_k^\dagger \hat{a}_k - \frac{1}{2}\right). \tag{2.2.23}$$

The summation of k in the Fourier transformation depends on the total number and BC of fermions. If the periodic BC is imposed for the spin operator ($\hat{\boldsymbol{\sigma}}_{N+1} = \hat{\boldsymbol{\sigma}}_1$),

- when $\mathcal{M}$ =even,
  the BC of the fermion operator is the anti-periodic

  $$\hat{a}_{N+1} = -\hat{a}_1. \tag{2.2.24}$$

  Then, the summation is taken over $k = (2n-1)\pi/N$ for $-\frac{N}{2} + 1 \leq n \leq \frac{N}{2}$.

- When $\mathcal{M}$ =odd,
  the BC of the fermion operator is the periodic

$$\hat{a}_{N+1} = \hat{a}_1. \tag{2.2.25}$$

  Then, the summation is taken over $k = 2n\pi/N$ for $-\frac{N}{2} + 1 \leq n \leq \frac{N}{2}$.

For the anti-periodic BC of spin operator ($\hat{\boldsymbol{\sigma}}_{N+1} = -\hat{\boldsymbol{\sigma}}_1$), the relation between $\mathcal{M}$ and the summation of k becomes inverted. In this thesis, we omit a complete calculation and utilize a resulting energy-spectrum. The ground-state energy for periodic BC is

$$E_0^P = -\sum_{m=0(odd)}^{2N-1} \left[(1-\gamma)^2 + 4\gamma \sin^2\Big(\frac{m\pi}{2N}\Big)\right]^{\frac{1}{2}}, \tag{2.2.26}$$

for anti-periodic BC

$$E_0^{AP} = -\sum_{m=0(even)}^{2N-2} \left[(1-\gamma)^2 + 4\gamma \sin^2\Big(\frac{m\pi}{2N}\Big)\right]^{\frac{1}{2}}. \tag{2.2.27}$$

The first excited state energy for periodic BC is

$$E_1^P = 2(\gamma - 1) - \sum_{m=0(even)}^{2N-1} \left[(1-\gamma)^2 + 4\gamma \sin^2\Big(\frac{m\pi}{2N}\Big)\right]^{\frac{1}{2}}. \tag{2.2.28}$$

From Eq.(2.2.27) and Eq.(2.2.28), we obtain the energy-crossing equation

$$E_1^P = E_0^{AP} + 2(\gamma - 1). \tag{2.2.29}$$

The two energies with different BCs cross at the transition point ($\gamma = 1$) with no FSC, which agrees with the result from the duality transformation. In our method, we carry out the extension of the equation of the energy-crossing (Eq.(2.2.29)) to the BA XXZ model. In the next section, we confirm that the same energy-crossing occurs in 2D Ising universality class.

2.3 Free Fermion Field Theory

We verify the energy crossing from the conformal field theory (CFT). By taking the continuous limit, the critical 2D Ising model is described by free fermion field (Appendix B),

$$S = \frac{1}{8\pi} \int dz d\bar{z} \left(\psi(z)\bar{\partial}\psi(z) + \bar{\psi(z)}\partial\bar{\psi(z)}\right), \tag{2.3.1}$$

where $\partial = \frac{\partial}{\partial z}, \bar{\partial} = \frac{\partial}{\partial \bar{z}}$. The fermion field has the anti-commutation relation $\{\psi(z), \psi(z')\} = \delta(z - z')$. The ψ is a primary field that satisfies

$$\langle \psi(z)\psi(w) \rangle = \frac{1}{z-w}. \tag{2.3.2}$$

The mode expansion is

$$i\psi(z) = \sum_k \psi_k z^{-k-\frac{1}{2}}. \tag{2.3.3}$$

Inverting Eq.(2.3.3)), we get

$$\psi_n = \oint \frac{dz}{2\pi i} z^{n-1/2} i\psi(z). \tag{2.3.4}$$

The modes have anti-commutation relation,

$$\begin{aligned}
\{\psi_n, \psi_m\} &= i^2 \left[\oint \frac{dz}{2\pi i}, \oint \frac{dw}{2\pi i} \right] z^{n-1/2} w^{m-1/2} \psi(z)\psi(w) \\
&= - \oint \frac{dw}{2\pi i} w^{m-1/2} \oint \frac{dz}{2\pi i} z^{n-1/2} \frac{-1}{z-w} \\
&= \oint \frac{dw}{2\pi i} w^{m-1/2} w^{n-1/2} = \delta_{n,m}.
\end{aligned} \tag{2.3.5}$$

If the summation is taken over half-odd integers ($k \in \mathbb{Z} + \frac{1}{2}$), the field has periodic BC,

$$\psi(\mathrm{e}^{2\pi i} z) = \psi(z), \bar{\psi}(\mathrm{e}^{2\pi i} \bar{z}) = \bar{\psi}(\bar{z}), \tag{2.3.6}$$

which correspond to $g = 1$ in the TFI model Eq.(2.2.1). If taken integers ($k \in \mathbb{Z}$), the field has anti-periodic BC,

$$\psi(\mathrm{e}^{2\pi i} z) = -\psi(z), \bar{\psi}(\mathrm{e}^{2\pi i} \bar{z}) = -\bar{\psi}(\bar{z}), \tag{2.3.7}$$

which yields $g = 1$.

In general, the excitation energy relates to the scaling dimension x_n of the scaling operators of the theory,

$$E_n - E_0 = \frac{2\pi}{L} \left(x_n + O(1/L) \right). \tag{2.3.8}$$

From operator product expansion for anti-periodic BC (Appendix C.2), the scaling dimension x is $1/8$,

$$E_0^{AP} - E_0^P = \frac{2\pi}{L} \left(\frac{1}{8} + O(1/L) \right). \tag{2.3.9}$$

For periodic BC, the scaling dimension of the 1-st excited energy has a same value,

$$E_1^P - E_0^P = \frac{2\pi}{L} \left(\frac{1}{8} + O(1/L) \right). \tag{2.3.10}$$

Therefore, the energies for the two BCs cross at the transition point,

$$E_1^P = E_0^{AP} + O(1/L). \tag{2.3.11}$$

2.4 Bond-Alternating XXZ chain

In this section, we introduce suitable BCs of the BA XXZ model and propose a new method to calculate a 2D Ising universality class transition point.

2.4.1 Boundary Conditions

To demonstrate analogous energy-crossing in the BA XXZ model, we introduce two types of twisted boundary conditions. One is a z-axis twisted boundary condition (zTBC)

$$S^x_{N+1} = -S^x_1, S^y_{N+1} = -S^y_1, S^z_{N+1} = S^z_1. \tag{2.4.1}$$

The spin rotational symmetry and spin reversal symmetry are conserved, but the translational symmetry is broken. The other is a y-axis twisted boundary condition (yTBC)

$$S^x_{N+1} = -S^x_1, S^y_{N+1} = S^y_1, S^z_{N+1} = -S^z_1. \tag{2.4.2}$$

The spin reversal symmetry is conserved, but the translational symmetry and spin rotational symmetry are broken. However, the Hamiltonian is invariant under the spin π-rotation

$$\hat{U}^z_\theta = \exp\left(i\pi \sum_j \hat{S}^z_j\right) \tag{2.4.3}$$

whose eigenvalue is a parity of magnetization

$$P_M = \exp\left(i\pi M\right) = (-1)^M. \tag{2.4.4}$$

The translational symmetry is broken by yTBC. Instead, the Hamiltonian has the following twist translation symmetry, as follows. By π-rotation for the N-th spin around y-axis, the twisted boundary is shifted to the bond between the N-th and $N-1$-th sites.

$$\begin{aligned} \mathrm{e}^{i\pi\hat{S}^y_N}\hat{H}(\mathrm{e}^{i\pi\hat{S}^y_N})^{-1} =& \cdots + (1+\delta)\left(-\hat{S}^x_{N-1}\hat{S}^x_N + \hat{S}^y_{N-1}\hat{S}^y_N - \Delta\hat{S}^z_{N-1}\hat{S}^z_N\right) \\ &+ (1-\delta)\left(\hat{S}^x_N\hat{S}^x_1 + \hat{S}^y_N\hat{S}^y_1 + \Delta\hat{S}^z_N\hat{S}^z_1\right). \end{aligned} \tag{2.4.5}$$

Then, operating the one-site translation, we obtain the original Hamiltonian

$$\hat{T}_R\mathrm{e}^{i\pi\hat{S}^y_N}\hat{H}(\hat{T}_R\mathrm{e}^{i\pi\hat{S}^y_N})^{-1} = \hat{H} \tag{2.4.6}$$

2.4.2 Anisotropic Limit for S=1/2

In the anisotropic limit, the S=1/2 BA XXZ model (Eq.(1.2.1)) is identical to the TFI model [20]. The zTBC and yTBC correspond to $g = \pm 1$ of the TFI model, respectively. Separating the Hamiltonian (Eq.(1.2.1)) to even and odd bonds,

$$\begin{aligned}\hat{H} = \beta \sum_{j}^{N/2} \left(\hat{S}^x_{2j} \hat{S}^x_{2j+1} + \hat{S}^y_{2j} \hat{S}^y_{2j+1} + \Delta \hat{S}^z_{2j} \hat{S}^z_{2j+1} \right) \\ + \sum_{j}^{N/2} \left(\hat{S}^x_{2j-1} \hat{S}^x_{2j} + \hat{S}^y_{2j-1} \hat{S}^y_{2j} + \Delta \hat{S}^z_{2j-1} \hat{S}^z_{2j} \right). \end{aligned} \tag{2.4.7}$$

We have defined the prefactor $\beta = \frac{1-\delta}{1+\delta}$. We firstly start with PBC. We take the anisotropic limit $\Delta \to \infty$ with a constraint $\Delta\beta \sim O(1)$. In this constraint, the bond-alternating parameter becomes infinitesimal, $\beta \to 0$. The largest contributions are the divergent term, $H_0 \equiv \sum \Delta \hat{S}^z_{2j-1} \hat{S}^z_{2j}$, which is regard as an unperturbed Hamiltonian. This unperturbed Hamiltonian is composed of $N/2$ isolated two spins $\hat{h}_j = \hat{S}^z_{2j-1} \hat{S}^z_{2j}$, whose ground-state is

$$\begin{aligned} |\uparrow_{2j-1} \downarrow_{2j}\rangle &= |\uparrow_j\rangle', \\ |\downarrow_{2j-1} \uparrow_{2j}\rangle &= |\downarrow_j\rangle'. \end{aligned} \tag{2.4.8}$$

We regard this two state as effective spin states. The effective states and operators are denoted by $'$. Therefore, the ground-state of H_0 is the $2^{N/2}$-fold degenerate. To the first order, the effective Hamiltonian becomes

$$\begin{aligned}\hat{H}_1 =& \sum_{j}^{N/2} \left(\beta \Delta \hat{S}^z_{2j} \hat{S}^z_{2j+1} \right) + \sum_{j}^{N/2} \left(\hat{S}^x_{2j-1} \hat{S}^x_{2j} + \hat{S}^y_{2j-1} \hat{S}^y_{2j} \right) \\ =& \sum_{j}^{N/2} \left(\beta \Delta \hat{S}^z_{2j} \hat{S}^z_{2j+1} \right) + \frac{1}{2} \sum_{j}^{N/2} \left(\hat{S}^+_{2j-1} \hat{S}^-_{2j} + \hat{S}^-_{2j-1} \hat{S}^+_{2j} \right). \end{aligned} \tag{2.4.9}$$

The quantum states defined in Eq.(2.4.8) satisfy

$$\hat{S}^z_{2j} |\uparrow_j\rangle' = -\frac{1}{2} |\uparrow_j\rangle', \tag{2.4.10}$$

$$\hat{S}^z_{2j} |\downarrow_j\rangle' = \frac{1}{2} |\downarrow_j\rangle', \tag{2.4.11}$$

$$\hat{S}^z_{2j+1} |\uparrow_{j+1}\rangle' = \frac{1}{2} |\uparrow_{j+1}\rangle', \tag{2.4.12}$$

$$\hat{S}^z_{2j+1} |\downarrow_{j+1}\rangle' = -\frac{1}{2} |\downarrow_{j+1}\rangle'. \tag{2.4.13}$$

So, the first terms are regarded as $-\hat{S'}^z_j \hat{S'}^z_{j+1}$ in the effective space. For the second term, the quantum states satisfy

$$\hat{S}^+_{2j-1}\hat{S}^-_{2j}\left|\downarrow_j\right\rangle' = \left|\uparrow_j\right\rangle', \tag{2.4.14}$$

$$\hat{S}^-_{2j-1}\hat{S}^+_{2j}\left|\uparrow_j\right\rangle' = \left|\downarrow_j\right\rangle'. \tag{2.4.15}$$

Therefore, the second term, $\frac{1}{2}\left(\hat{S}^+_{2j-1}\hat{S}^-_{2j} + \hat{S}^-_{2j-1}\hat{S}^+_{2j}\right)$ is regarded as $\frac{1}{2}\left(\hat{S'}^+_j + \hat{S'}^-_j\right) = \hat{S'}^x_j$ in the effective space. The total effective Hamiltonian becomes

$$\hat{H}' = \sum_j^{N/2}\left(-\beta\Delta\hat{S'}^z_j\hat{S'}^z_{j+1} + \hat{S'}^x_j\right). \tag{2.4.16}$$

By operating $\exp\left(i\pi\sum_i^{N/2}\hat{S'}^z_j\right)$, the effective Hamiltonian becomes the TFI model,

$$\hat{H}' = \beta\Delta\sum_j^{N/2}\left(-\hat{S'}^z_j\hat{S'}^z_{j+1} - \frac{1}{\beta\Delta}\hat{S'}^x_j\right), \tag{2.4.17}$$

In zTBC, boundary terms are

$$-\hat{S}^x_N\hat{S}^x_1 - \hat{S}^y_N\hat{S}^y_1 + \hat{S}^z_N\hat{S}^z_1. \tag{2.4.18}$$

Because the x,y terms on 2j,2j+1-bond vanish in the anisotropic limit, the zTBC correspond to the periodic BC, $g = 1$. In yTBC, the boundary terms are

$$-\hat{S}^x_N\hat{S}^x_1 + \hat{S}^y_N\hat{S}^y_1 - \hat{S}^z_N\hat{S}^z_1. \tag{2.4.19}$$

The effect of yTBC survives after taking the limit. The z-direction term remains, $-\beta\Delta\hat{S}^z_N\hat{S}^z_1$ The yTBC corresponds to the anti-periodic BC $g = -1$. The relation of BC is summarized in Table.2.2.

BA XXZ anisotropy limit→	TFI
PBC	periodic
zTBC	periodic
yTBC	anti-periodic

Table 2.2: The correspondence of each BC

For S>1/2, the above perturbative discussion can be applied (Appendix D).

2.4.3 Method to Calculate the Transition Point

In the BA XXZ model, PBC and zTBC correspond to periodic BC of the TFI model. The yTBC correspond to anti-periodic BC. Since the energy crossing happens with

periodic and anti-periodic BCs, we can calculate the transition point by two methods. One is using PBC and yTBC :

$$E_0^{PBC}(M=0,U_\pi^y)=E_0^{yTBC}(M,U_\pi^y) \tag{2.4.20}$$

named yTBC-PBC method. The other is using zTBC and yTBC :

$$E_0^{zTBC}(M=0,U_\pi^y)=E_0^{yTBC}(M,U_\pi^y) \tag{2.4.21}$$

named yTBC-zTBC method. We can distinguish different phase by quantum numbers M, U_π^y, explained in Chap. 4.

2.4.4 Finite Size Correction

In general, there is an FSC in our methods, Eq.(2.4.20) and Eq.(2.4.21) in a region in $1<\Delta<\infty$, but vanishes on the anisotropic limit $\Delta\to\infty$. In the anisotropic limit, the zTBC and PBC of the BA XXZ model become periodic BC of the TFI model, and the yTBC becomes anti-periodic BC (Sec 2.4.2). So,our methods become identical to Eq.(2.2.29), that has no FSC for arbitrary spins. The larger Δ is, the smaller the FSC becomes.

Moreover, the FSC vanishes at the AT point. On the self dual line ($\delta=0$), the Hamiltonian with zTBC becomes

$$\begin{aligned}\hat{H}=\sum_j^{L-1}\left(\hat{S}_j^x\hat{S}_{j+1}^x+\hat{S}_j^y\hat{S}_{j+1}^y+\Delta\hat{S}_j^z\hat{S}_{j+1}^z\right)\\ -\hat{S}_L^x\hat{S}_1^x-\hat{S}_L^y\hat{S}_1^y+\Delta\hat{S}_L^z\hat{S}_1^z.\end{aligned} \tag{2.4.22}$$

We define π spin rotation at j site about z-axis as $\hat{u}_j^z=\exp(i\pi\hat{S}_j^z)$. Since the Hamiltonian (Eq.(2.4.22)) is invariant under $\hat{T}_R\hat{u}_L^z$ (proved in Sec 2.4.1),

$$\hat{T}_R\hat{u}_L^z\hat{H}\left|U_\pi^y\right\rangle=\hat{H}\hat{T}_R\hat{u}_L^z\left|U_\pi^y\right\rangle. \tag{2.4.23}$$

The commutation relation between $\hat{U}_\pi^y$ and $\hat{u}_L^z$ is

$$\begin{aligned}\hat{U}_\pi^y\hat{u}_L^z&=\exp(i\pi\sum_j\hat{S}_j^y)\exp(i\pi\hat{S}_L^z)\\&=\exp(-i\pi\hat{S}_L^z)\exp(i\pi\sum_j\hat{S}_j^y)\\&=\exp(-2i\pi\hat{S}_L^z)\hat{u}_L^z\hat{U}_\pi^y.\end{aligned} \tag{2.4.24}$$

When S is a half-integer, the eigenvalue of $\hat{S}_L^z$ is a half-integer, which yields

$$\hat{U}_\pi^y\hat{u}_L^z=-\hat{u}_L^z\hat{U}_\pi^y. \tag{2.4.25}$$

So,

$$\begin{aligned}\hat{U}_\pi^y \hat{T}_R \hat{u}_L^z \left|U_\pi^y = 1\right\rangle &= -\hat{T}_R \hat{u}_L^z \hat{U}_\pi^y \left|U_\pi^y = 1\right\rangle \\ &= -\hat{T}_R \hat{u}_L^z \left|U_\pi^y = 1\right\rangle \\ &\equiv -\left|U_\pi^y = -1\right\rangle . \end{aligned} \tag{2.4.26}$$

Consequently, $|U_\pi^y = 1\rangle$ and $|U_\pi^y = -1\rangle$ are degenerate for an arbitrary system-size N, that is

$$E_0^{zTBC}(L, M = 0, U_\pi^y = -1) = E_0^{zTBC}(L, M = 0, U_\pi^y = 1), \tag{2.4.27}$$

as one can see in Fig.4.1(a) at $\delta = 0$. And, at AT point, the isotropy makes the zTBC and yTBC identical. We replace the RHS of Eq.(2.4.27) by yTBC. The spin reversal U_π^y is replaced by the parity of magnetization P_M (recall Eq.(2.4.4)). Eq.(2.4.27) becomes

$$E_0^{zTBC}(L, M = 0, U_\pi^y = -1) = E_0^{yTBC}(L, M = even). \tag{2.4.28}$$

The absence of FSC in AT point gives the small FSC near AT point for an integer spin. The numerical results are presented in Chap. 4.

Chapter 3

2D Gaussian Universality Class

In this chapter, firstly, we discuss a free boson on a conformal field theory. Next, the BA XXZ model is transformed to a phase Hamiltonian by a bosonization method. The phase Hamiltonian has a free boson term and the others that break a U(1) symmetry. At last, by a perturbative renormalization calculation, it is certified that energies in the zTBC cross at a Gaussian universality transition point. The same discussion for the yTBC is a future task.

3.1 Free Boson Field theory

The action of a free boson field theory is

$$\hat{H} = \int \partial\phi(z,\bar{z})\bar{\partial}\phi(z,\bar{z}), \tag{3.1.1}$$

in other word, called a 2D Gaussian model. From the equations of motion

$$\partial\bar{\partial}\phi(z,\bar{z}) = 0, \bar{\partial}\partial\phi(z,\bar{z}) = 0, \tag{3.1.2}$$

we can decompose $\phi(z,\bar{z})$ into holomorphic and anti-holomorphic parts

$$\phi(z,\bar{z}) = \frac{1}{2}\left(\varphi(z) + \bar{\varphi}(\bar{z})\right). \tag{3.1.3}$$

The field $\varphi(z)$ is not a primary operator, but its derivative is a primary,

$$\partial\varphi(z)\partial\varphi(w) = -\frac{1}{(z-w)^2} + \cdots. \tag{3.1.4}$$

The mode expansion of the primary field is

$$i\partial\varphi(z) = \sum_n a_n z^{-n-1} \tag{3.1.5}$$

From the Noether theorem, the stress-energy tensor is expressed as

$$T(z) = -\frac{1}{2} : \partial\varphi(z)\partial\varphi(z) :, \tag{3.1.6}$$

where :: means a normal ordering. From the operator product expansion (OPE) of the stress-energy tensor,

$$T(z)T(w) = \frac{1/2}{(z-w)^4} + \frac{2T(w)}{(z-w)^2} + \frac{\partial T(w)}{z-w} + \text{regularparts}, \tag{3.1.7}$$

the central charge is $c = 1$. The OPE of the $T(z)$ and $\partial\varphi(z)$ is

$$T(z)\partial\varphi(w) = \frac{1}{(z-w)^2}\partial\varphi(w) + \frac{1}{z-w}\partial\partial\varphi(w) + reg, \tag{3.1.8}$$

which means that $\partial\varphi(w)$ is the primary field that has the conformal dimension $(1, 0)$. The vertex operator is defined as

$$\mathcal{V}_\alpha(z) =: \mathrm{e}^{i\alpha\varphi(z)} : \tag{3.1.9}$$

This field is primary and conformal weight is

$$h(\alpha) = \alpha^2 \tag{3.1.10}$$

From Appendix C.3, OPE of the vertex operators and $\partial\varphi(z)$ is

$$\partial\varphi(z)\mathcal{V}_{-\alpha}(w) = \frac{\alpha}{(z-w)}\mathcal{V}_\alpha(w) + \text{regularparts}. \tag{3.1.11}$$

The OPE of the vertex operators and the stress-energy tensor is

$$T(z)\mathcal{V}_{-\alpha}(w) = \frac{\alpha^2/2}{(z-w)^2}\mathcal{V}_\alpha(w) + \frac{1}{(z-w)}\partial_w\mathcal{V}_\alpha(w) + \text{regularparts}. \tag{3.1.12}$$

The OPE of the vertex operators is

$$\mathcal{V}_\alpha(z)\mathcal{V}_{-\alpha}(w) = \frac{1}{(z-w)^{2\alpha^2}}\mathcal{V}_{-\alpha}(w). \tag{3.1.13}$$

3.2 Bosonization

For S=1/2, the spin Hamiltonian (Eq.(1.2.1)) can be transformed to the following phase Hamiltonian [21] [22] (Appendix E)

$$\hat{H} = \int dx \left[A\left(\nabla\theta(x)\right)^2 + Cp(x)^2 - B\cos\theta(x) + D\cos 2\theta(x)\right]. \tag{3.2.1}$$

The p is the momentum density conjugate to θ

$$[\theta(x), p(x')] = i\delta(x - x'). \tag{3.2.2}$$

The constants A, B, C, D are evaluated as

$$A = \frac{Ja}{8\pi}\left(1 + \frac{3\Delta}{\pi}\right), \tag{3.2.3}$$

$$C = 2\pi Ja\left(1 - \frac{\Delta}{\pi}\right), \tag{3.2.4}$$

$$B = \frac{J\delta}{a}, \tag{3.2.5}$$

$$D = \frac{\pi^2 \Delta J}{8a}. \tag{3.2.6}$$

When $B = 0, D = 0$, Eq.(3.2.1) is the Gaussian model.

3.3 Around the Gaussian fixed point

We shortly review a perturbative renormalization calculation by Kitazawa[8]. We consider the perturbation around the Gaussian fixed point

$$H = H_0 + \lambda \int_0^L dx \mathcal{O}_1. \tag{3.3.1}$$

Here, $H_0 = \int dx (\nabla\theta)^2$. The H_0 is the Gaussian fixed point Hamiltonian and $\mathcal{O}_1$ is the scaling operator that has scaling dimension x_1. Up to the first order perturbation, the excitation energies are [24]

$$E_n - E_0 = \frac{2\pi}{L}\left(x_n + 2\pi\lambda C_{n1n}\left(\frac{2\pi}{L}\right)^{x_1 - 2}\right). \tag{3.3.2}$$

The x_n is scaling dimension of the operator $\mathcal{O}_n$. The C_{n1n} is the coefficient of the operator product expansion (OPE),

$$\mathcal{O}_1(z, \bar{z})\mathcal{O}_n(0,0) = C_{n1n}\left(\frac{\alpha}{z}\right)^{h_1}\left(\frac{\alpha}{\bar{z}}\right)^{\bar{h}_1}\mathcal{O}_n(0,0) + \cdots, \tag{3.3.3}$$

h_1 and $\bar{h}_1$ are the conformal weight of $\mathcal{O}_1$. In the zTBC, we consider the following operators [8]

$$\mathcal{O}_1 = \sqrt{2}\cos\sqrt{2}\theta, \tag{3.3.4}$$

$$\mathcal{O}^e_{1/2} = \sqrt{2}\cos\frac{1}{\sqrt{2}}\theta, \tag{3.3.5}$$

$$\mathcal{O}^o_{1/2} = \sqrt{2}\sin\frac{1}{\sqrt{2}}\theta \tag{3.3.6}$$

Using the OPE of the vertex operators Eq.(3.1.13), we can calculate the OPE of $\mathcal{O}^e_{1/2}$,$\mathcal{O}^o_{1/2}$ and $\mathcal{O}_1$

$$\mathcal{O}_1(z,\bar{z})\mathcal{O}^e_{1/2}(0,0) = \frac{\sqrt{2}}{2}\left(\frac{\alpha}{z}\right)^{K/4}\left(\frac{\alpha}{\bar{z}}\right)^{K/4}\mathcal{O}^e_{1/2}(0,0) + \cdots, \tag{3.3.7}$$

$$\mathcal{O}_1(z,\bar{z})\mathcal{O}^o_{1/2}(0,0) = -\frac{\sqrt{2}}{2}\left(\frac{\alpha}{z}\right)^{K/4}\left(\frac{\alpha}{\bar{z}}\right)^{K/4}\mathcal{O}^o_{1/2}(0,0) + \cdots, \tag{3.3.8}$$

where $K = (B/A)^{1/2}$. From Eq.(3.3.2), the excitation energies are

$$E_1(\pi) - E_0(0) = \frac{2\pi}{L}\left(\frac{K}{8} + 2\pi\lambda\frac{\sqrt{2}}{2}\left(\frac{2\pi}{L}\right)^{K/2-2} + \cdots\right), \tag{3.3.9}$$

$$E_2(\pi) - E_0(0) = \frac{2\pi}{L}\left(\frac{K}{8} - 2\pi\lambda\frac{\sqrt{2}}{2}\left(\frac{2\pi}{L}\right)^{K/2-2} + \cdots.\right) \tag{3.3.10}$$

Then, the two energies are crossing at the transition point, $\lambda = 0$.

Chapter 4

Numerical Calculation

We numerically study the 2D Ising and the 2D Gaussian universality transition points of the BA XXZ model for S=1/2,1,3/2

$$\hat{H}(\delta,\Delta)=\sum_{j}^{N}\left[1-(-1)^{j}\delta\right]\left(\hat{S}_{j}^{x}\hat{S}_{j+1}^{x}+\hat{S}_{j}^{y}\hat{S}_{j+1}^{y}+\Delta\hat{S}_{j}^{z}\hat{S}_{j+1}^{z}\right). \tag{1.2.1}$$

Using our method, we can calculate transition points near a multicritical point with a small FSC. The energy is calculated by the exact diagonalization using Lanczos method[25] (see Appendix F).

4.1 $S = 1/2$

In this section, the numerical results for S=1/2 are shown. The transition lines are calculated by the proposed method. Critical exponents are also calculated. The value of numerical result corresponds to the 2D Ising type precisely.

4.1.1 Phase diagram

The 2D Gaussian transition line is $\delta = 0$ ($\Delta \leq 1$), that can be obtained exactly[8]. We numerically calculate the 2D Ising transition line, with yTBC-PBC method (Eq.(2.4.20)) and yTBC-zTBC method (Eq.(2.4.21)). To search the energy crossing point, we are fixing Δ and varying δ (Fig.4.1(a)). The phase diagram is shown in Fig.4.2(a). The 2D Gaussian universality transition line bifurcates into the two 2D Ising universality transition lines at $(\Delta = 1, \delta = 0)$. The AT point, $\Delta = 1, \delta = 0$, is a BKT transition point where the correlation length diverges singularly. In large Δ, the size dependence is small (Fig.4.3(a)). The value of crossing points δ_c almost converge even in the finite-size numerical calculations. Near the AT point, two 2D Ising universality transition lines are exceedingly close. This effect makes the FSC bigger in the yTBC-PBC method, but still small in the yTBC-zTBC method (Fig.4.3(b)). The value $\delta_c(\infty)$ is obtained by an extrapolation. We set the fitting function $\delta_c(N) = a\exp(-N/b) + \delta_c(\infty)$, with a

and b being fitting constants. To measure the FSC when Δ approaches the AT point, we calculate a variation of crossing point, $D(N_1, N_2) \equiv |\delta_c(N_1) - \delta_c(N_2)|$. In Fig.4.4, $D(24, 22)$ is shown. The two methods are identical in $\Delta \to \infty$. Near the AT point, the size dependence is much smaller in yTBC-zTBC method than yTBC-PBC method. From another point of view, the slope of size dependence is positive in yTBC-zTBC method and negative in yTBC-PBC method. So, we can determine the error bar using the numerical results for the largest system, shown in Fig.4.2(b).

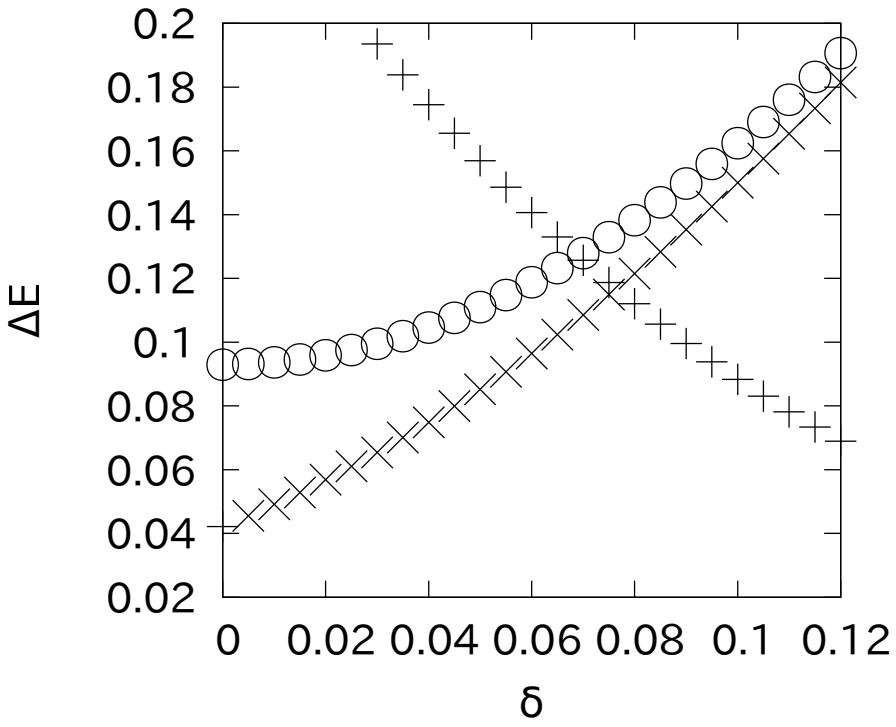

(a)

Figure 4.1: (a): The energy spectrum for $\Delta = 2.0, N = 14$. The value of each energy E minus E_0^{PBC}, denoted by ΔE, is plotted. ◯ is E_1^{PBC}, $\times$ is E_1^{zTBC}, $+$ is E_0^{yTBC}.

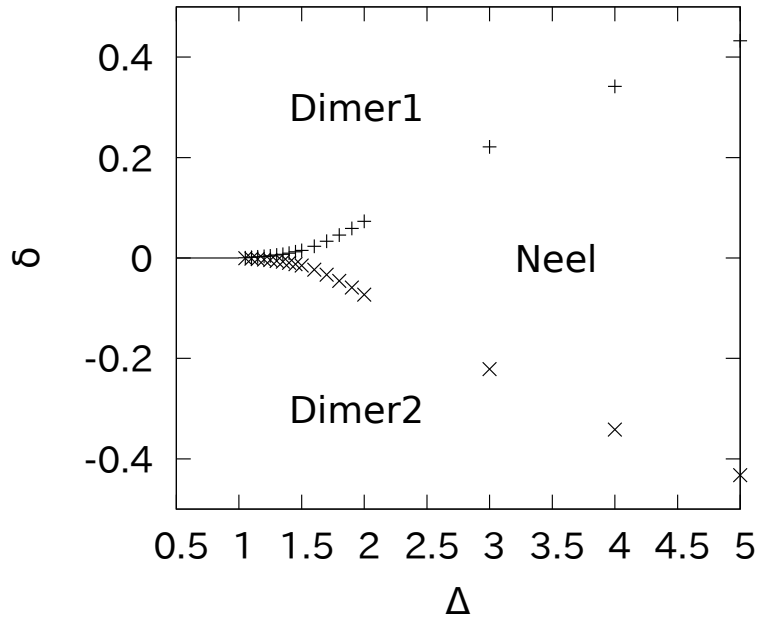

(a)

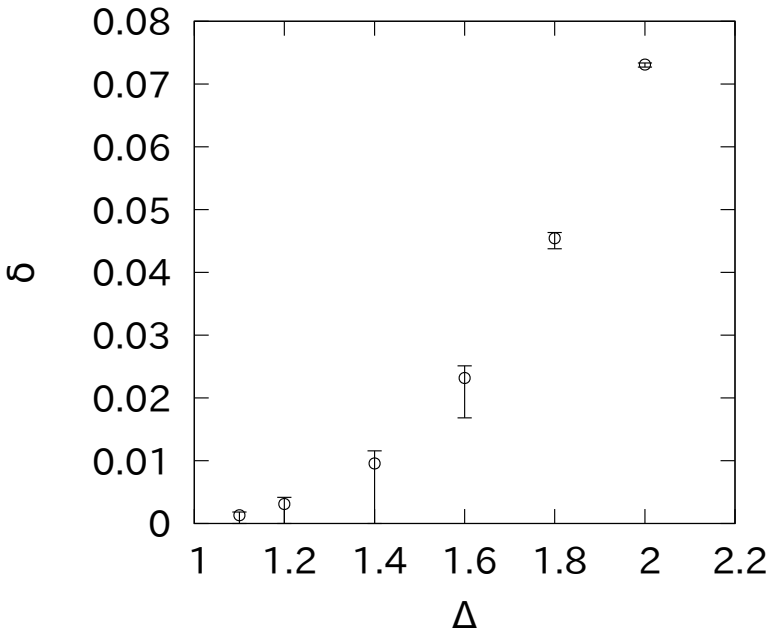

(b)

Figure 4.2: (a): The phase diagram using the data of N=24. The 2D Gaussian transition line is exactly obtained, and the 2D Ising transition lines are calculated by yTBC-zTBC method. (b): The enlarged view of (a) near the AT point with the error bar. The error range is smaller in larger Δ.

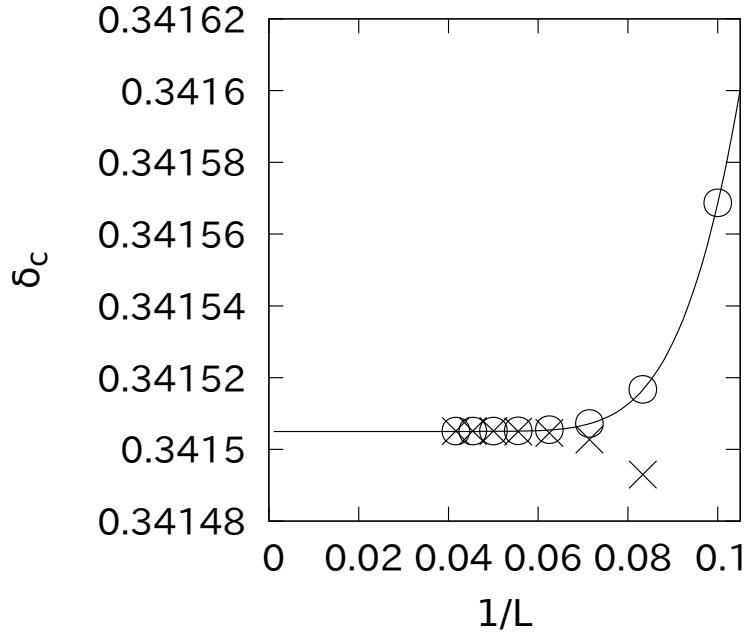

(a)

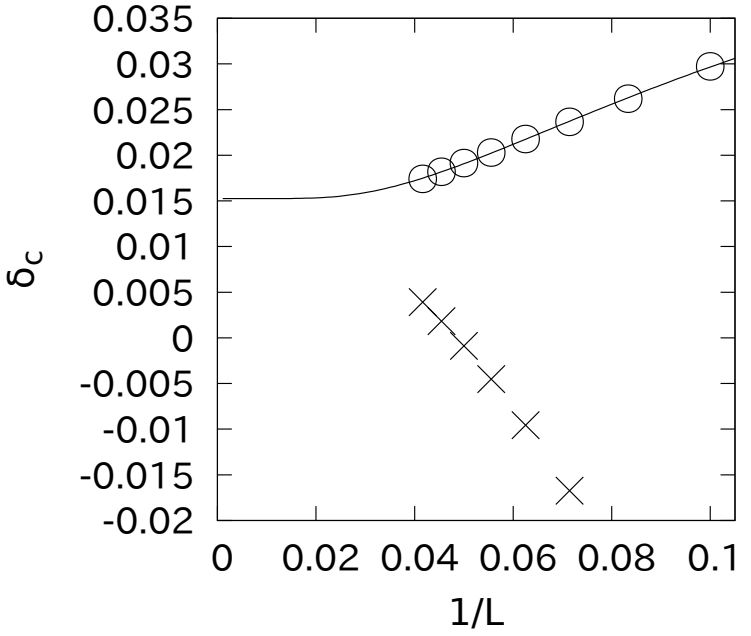

(b)

Figure 4.3: (a),(b): The FSC of a crossing point δ_c to a inverse system size $1/N$ respectively for $\Delta = 4.0, 1.5$. The $\circ$ and $\times$ are the results of the yTBC-zTBC and yTBC-PBC method. Solid lines show the extrapolation.

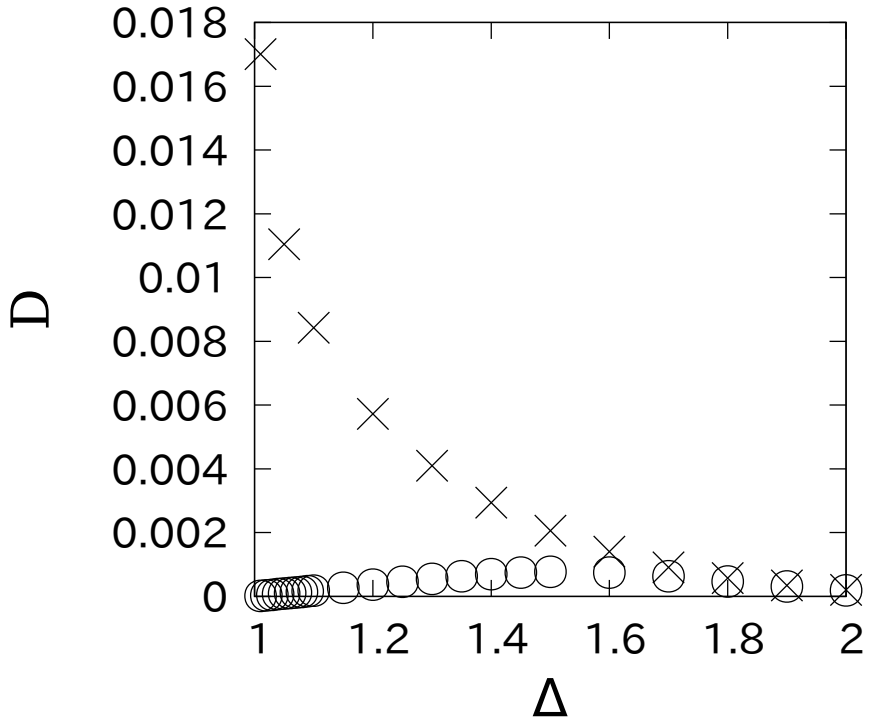

Figure 4.4: (b): The variation of the FSC, $D(N_1 = 24, N_2 = 22)$. The $\circ$ and $\times$ are yTBC-zTBC and yTBC-PBC method.

4.1.2 Critical exponent

To confirm the universality class of the resulting transition point, we calculate critical exponents, scaling dimensions and a central charge.

PBC — The scaling behavior of the ground state is related to central charge c, [23]

$$E_0(M=0, U_\pi^y = (-1)^{N/2}, N) = N\epsilon_\infty - \frac{\pi v c}{6N}, \tag{4.1.1}$$

where ϵ_∞ is the ground-state energy density for $N = \infty$ and v is the spin wave velocity. The scaling dimension x_n is calculated by excited energy, [24]

$$E_n(M=0,N) - E_0(M=0,N) = \frac{x_n 2\pi v}{N}. \tag{4.1.2}$$

The spin wave velocity is calculated numerically

$$v = \frac{E(M=0, U_\pi^y = -(-1)^{N/2}, q = 2\pi/N) - E_0(M=0, U_\pi^y = -(-1)^{N/2}, q=0)}{2\pi/N}. \tag{4.1.3}$$

The numerical result of the central charge is shown in Fig.4.5. Far from AT point,$\Delta = 4.0$, the extrapolated value of c is 0.500143, which is close to the expected value $c = 1/2$. Because Eq.(4.1.1) and Eq.(4.1.2) are affected from the multicritical point directly, the value of c has larger FSC near the AT point, $\Delta = 1.5$. The scaling dimensions x_n are shown in Fig.4.6. The expective values are $x_1 = 1/8$ and $x_2 = 1$. The values of scaling dimension have larger FSC near the AT point. The size dependence of x_2 is not monotonous, that makes the extrapolation difficult.

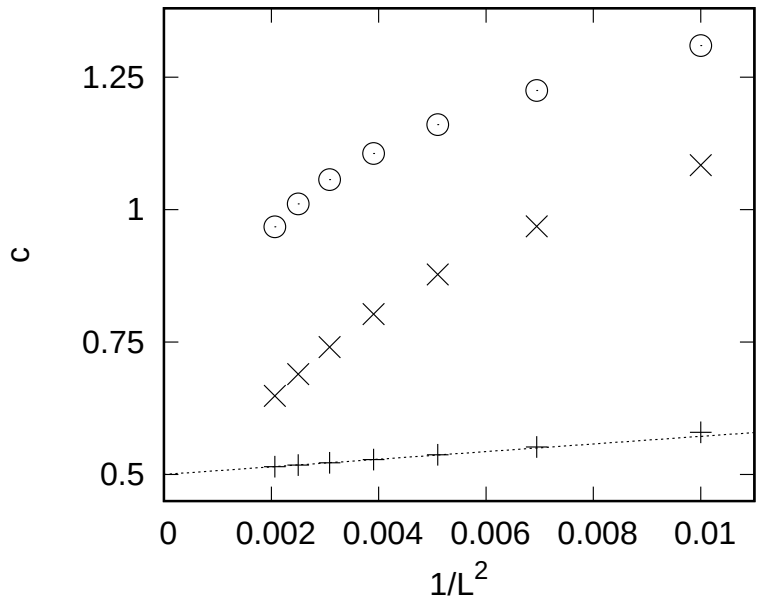

Figure 4.5: The central charge of the resulting transition point. The $+, \times, \odot$ are respectively $\Delta = 4.0, 2.0, 1.7$

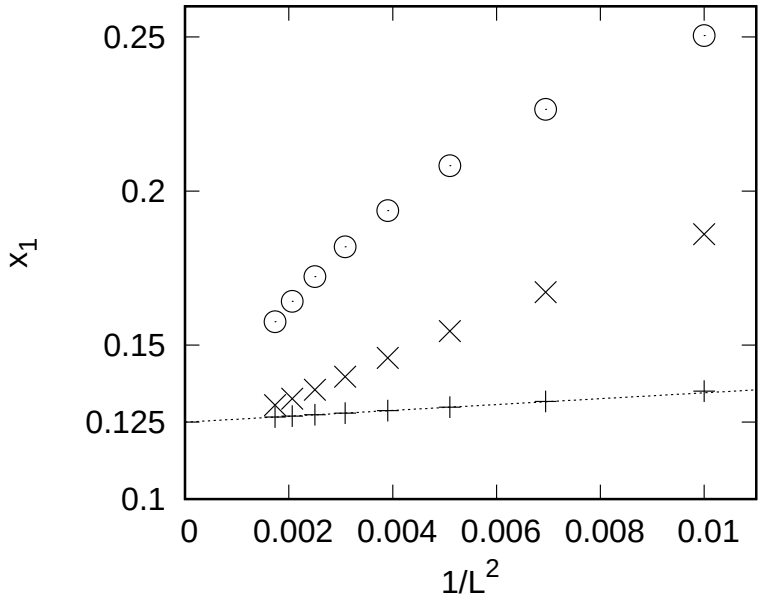

(a)

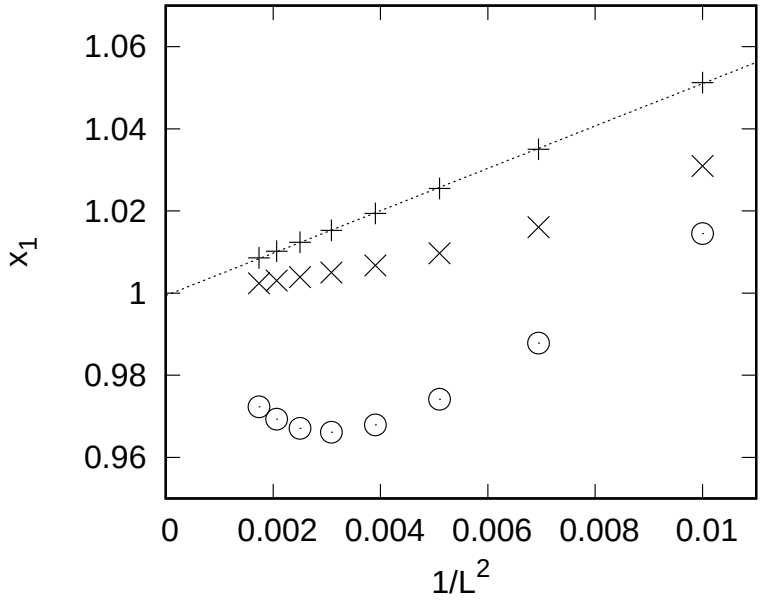

(b)

Figure 4.6: The scaling dimension of the resulting transition point. The $+, \times, \odot$ are respectively $\Delta = 4.0, 2.0, 1.7$

zTBC — Because the zTBC of the S=1/2 BA XXZ chain corresponds to the periodic BC of the 2D Ising model (Sec 2.4.2), an expective value of scaling dimensions are $x_1 = 1/8, x_2 = 1$ The numerical results are shown in Fig.4.7. The result has a close value to expected value of periodic Ising model.

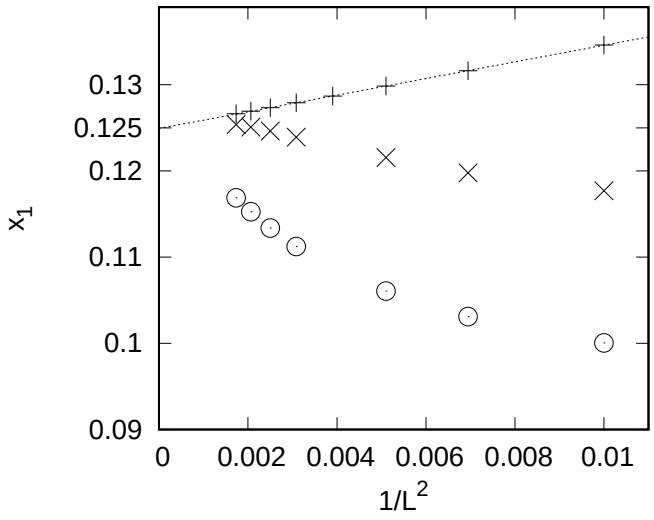

(a)

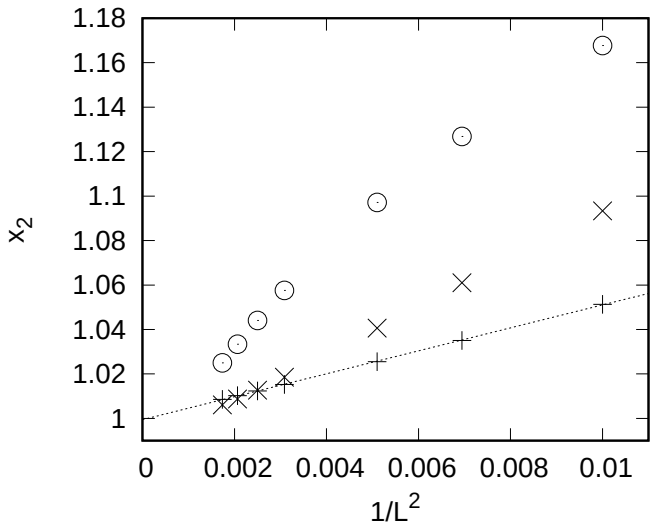

(b)

Figure 4.7: The scaling dimension $+, \times, \odot$ are respectively $\Delta = 4.0, 2.0, 1.7$.

yTBC — Since the yTBC corresponds to the anti-periodic BC of the 2D Ising model (Sec 2.4.2), the expective value of scaling dimensions are $x_1 = 1/8, x_2 = 1/2$. In the calculation of the critical exponent in the yTBC, we use the energies that have an even magnetization, M =even, since the ground state in the anisotropic limit, Eq.(2.4.8), has an even magnetization. The numerical results are shown in Fig.4.8. The result has a close value to expected value of anti-periodic Ising model.

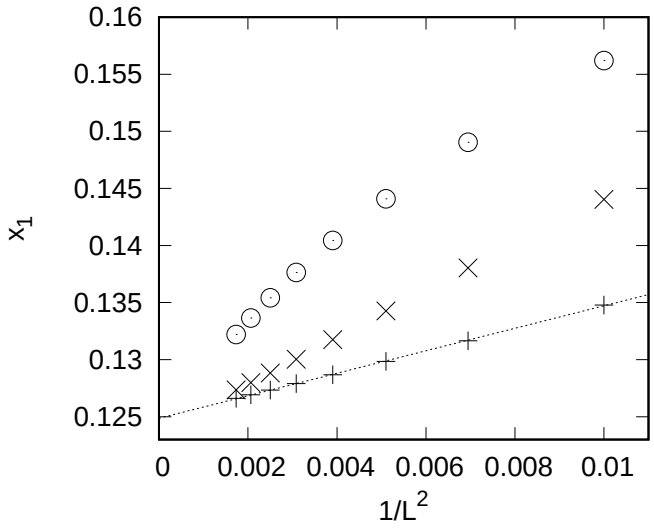

(a)

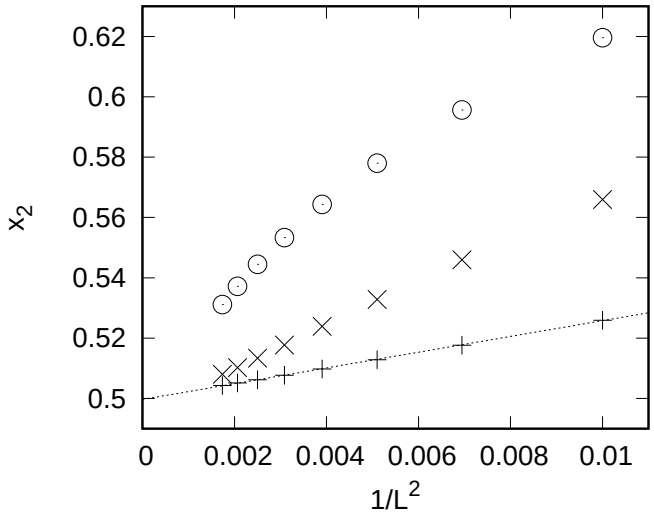

(b)

Figure 4.8: The scaling dimension $+, \times, \odot$ are respectively $\Delta = 4.0, 2.0, 1.7$

4.2 $S = 1$

Haldane[9] predicted about the energy gap of the Heisenberg chain for integer and half-odd integer spin. The integer spin has gapless ground-state. The half-odd integer spin has gapped ground-state. This prediction has been verified by many researches numerically [26] [27] and analytically [6] [28].

A valence bond solid (VBS) state, defined later, has a different quantum number depending on the BC. We can determine a boundary between different VBS phases. The S=1 spin can take $S_z = 1, 0, -1$ states, so the dimension of the Hilbert space is 3^N. The numerical calculation is restricted to a smaller system than S=1/2. By our method, we obtain a phase diagram with a small FSC.

4.2.1 Valence Bond Solid

In the isolated case, $\delta = 1$, the ground-state is exactly a singlet of S=1 spin. And, the Heisenberg point, $\Delta = 1, \delta = 0$, belongs to a Haldane phase according to his conjecture. These phase are called a VBS phase. The difference of each phase is a pairing of a singlet of divided S=1/2 spins. The S=1 spin can be divided into two S=1/2 spins. There are a few ways to take the singlet pairing of the divided S=1/2 spins (Fig.4.9 (a)(b)(c)). The VBS state with PBC can be written[29][30] by Schwinger bosons representation,

$$\begin{aligned} |S, m, PBC\rangle = & \left(a_N^\dagger b_1^\dagger - b_N^\dagger a_1^\dagger\right)^{S-m} \\ & \times \prod_{j=1}^{N/2-1} \left(a_{2j-1}^\dagger b_{2j}^\dagger - b_{2j-1}^\dagger a_{2j}^\dagger\right)^{S+m} \\ & \times \left(a_{2j}^\dagger b_{2j+1}^\dagger - b_{2j}^\dagger a_{2j+1}^\dagger\right)^{S-m} \\ & \times \left(a_{N-1}^\dagger b_N^\dagger - b_{N-1}^\dagger a_N^\dagger\right)^{S+m} |0\rangle \,, \end{aligned} \tag{4.2.1}$$

where $-S \leq m \leq S$, and $a_j^\dagger$ ($b_j^\dagger$) creates the $S = 1/2 \uparrow (\downarrow)$ spin at the j-th site. The $|0\rangle$ is a state where no spin exist. The spin reversal symmetry of this state is $U_\pi^y = (-1)^{SN-S+m}$. The dimer1, Haldane and dimer2 state are $|S = 1, m = 1, 0, -1\rangle$ respectively. Under the zTBC, the m-VBS state changes[31] to

$$\begin{aligned} |S, m, zTBC\rangle = & \left(a_N^\dagger b_1^\dagger + b_N^\dagger a_1^\dagger\right)^{S-m} \\ & \times \prod_{j=1}^{N/2-1} \left(a_{2j-1}^\dagger b_{2j}^\dagger - b_{2j-1}^\dagger a_{2j}^\dagger\right)^{S+m} \\ & \times \left(a_{2j}^\dagger b_{2j+1}^\dagger - b_{2j}^\dagger a_{2j+1}^\dagger\right)^{S-m} \\ & \times \left(a_{N-1}^\dagger b_N^\dagger - b_{N-1}^\dagger a_N^\dagger\right)^{S+m} |0\rangle \,, \end{aligned} \tag{4.2.2}$$

that has $U_\pi^y = (-1)^{SN-S+m}$. Under the yTBC, the m-VBS state changes to

$$\begin{aligned}|S,m,yTBC\rangle = &\left(a_N^\dagger a_1^\dagger + b_N^\dagger b_1^\dagger\right)^{S-m} \\ &\times \prod_{j=1}^{N/2-1}\left(a_{2j-1}^\dagger b_{2j}^\dagger - b_{2j-1}^\dagger a_{2j}^\dagger\right)^{S+m} \\ &\times \left(a_{2j}^\dagger b_{2j+1}^\dagger - b_{2j}^\dagger a_{2j+1}^\dagger\right)^{S-m} \\ &\times \left(a_{N-1}^\dagger b_N^\dagger - b_{N-1}^\dagger a_N^\dagger\right)^{S+m}|0\rangle\,, \end{aligned} \tag{4.2.3}$$

that has $U_\pi^y = (-1)^{SN-S+m}$. Only the first factor $\left(a_N^\dagger a_1^\dagger + b_N^\dagger b_1^\dagger\right)^{S-m}$ changes the parity of the magnetization,

$$\left(a_N^\dagger a_1^\dagger + b_N^\dagger b_1^\dagger\right)|M = even, odd\rangle = |M = odd, even\rangle\,. \tag{4.2.4}$$

Therefore, if $S-m$ is even (odd), the VBS state $|S,m,yTBC\rangle$ has even (odd) magnetization. The quantum numbers for each BC are summarized in Table.4.1. We can determine the phase boundary of the VBS phase by the parity of the magnetizaton in yTBC.

	dimer1	Haldane	dimer2
PBC	(0,-1)	(0,-1)	(0,-1)
zTBC	(0,1)	(0,-1)	(0,1)
yTBC	(even,1)	(odd,-1)	(even,1)

Table 4.1: Quantum number (M,U_π^y) for $S = 1$.

4.2.2 Phase diagram

For S=1, the disorder phases are dimer1, dimer2 and Haldane phase. The transition between Néel phase and disorder phase is the 2D Ising universality class. The transition between different disorder phases is the 2D Gaussian universality class. The phase diagram is shown in Fig.4.9(d). Because the yTBC and zTBC become identical at the isotropic point, numerical results of 2D Ising and 2D Gaussian for a finite system size transition lines cross exactly.

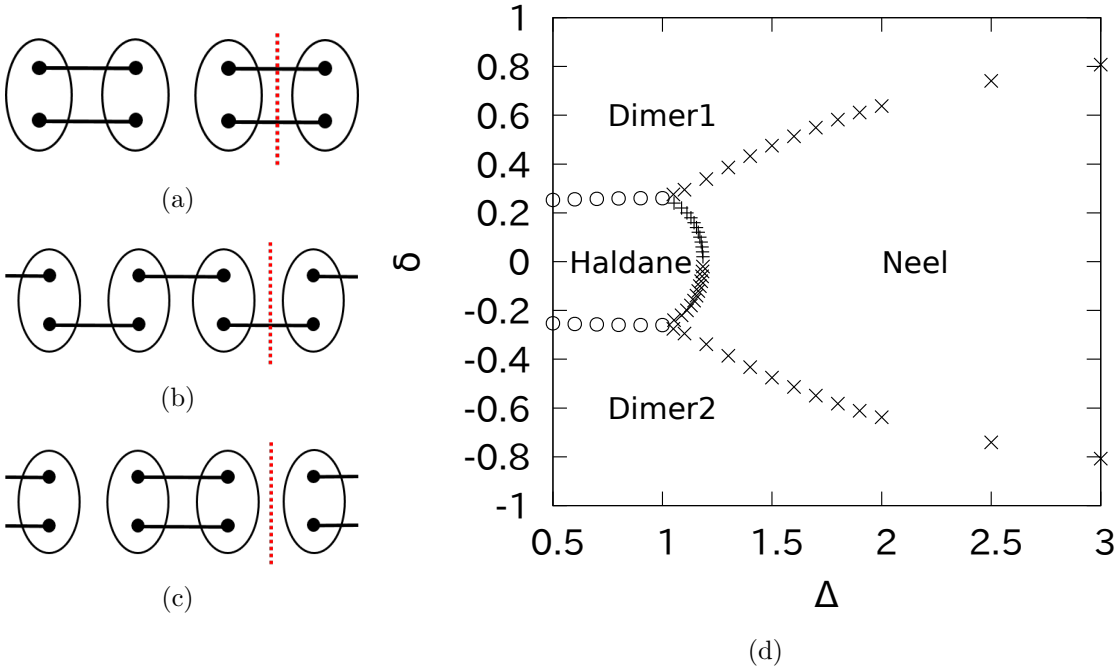

Figure 4.9: (a),(b),(c) : The VBS state for S=1 taking the different singlet pairing. Respectively dimer1, Haldane and dimer2 state. Dashed lines denote the boundary. (d) : The phase diagram for S=1. The numerical result agree with the Haldane conjecture. The transition line between dimer1,2 and Néel belongs to the 2D Ising universality. And, the one between dimer1 and dimer2 is the 2D Gaussian universality.

2D Ising universality

The size dependence for Dimer-Néel transition is shown in Fig.4.10. Similar to the case for S=1/2, the yTBC-zTBC method has a smaller FSC than the yTBC-PBC method. The size dependence for Haldane-Néel transition is shown in Fig.4.11. The case for $\delta = 0$ is widely studied. The 2D Ising transition point was calculated by several researches [32, 33, 34, 35]. Our result is $\Delta_c = 1.1856 \pm 0.0002$, highly accurate than those of previous researches.

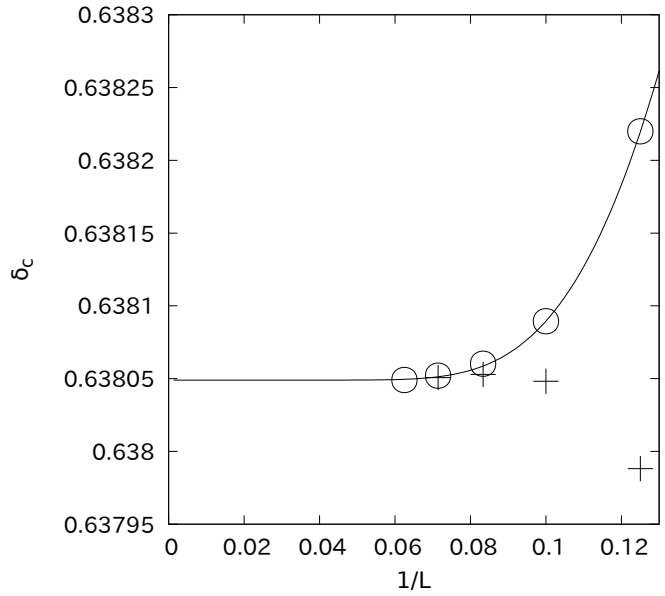

(a)

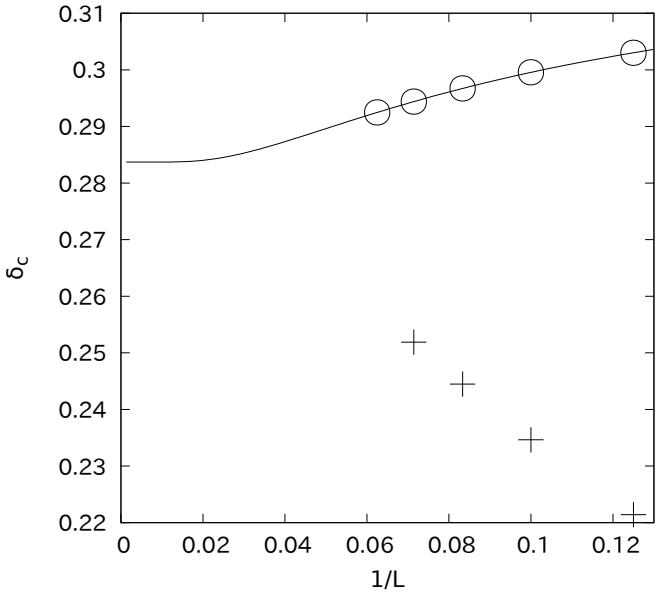

(b)

Figure 4.10: (a),(b): The FSC of a crossing point δ_c for a S=1 dimer-Néel transition to a inverse system size $1/N$ respectively for $\Delta = 2.0, 1.1$. The $\circ$ and $+$ are the result of the yTBC-zTBC and yTBC-PBC method. Solid line shows the extrapolation.

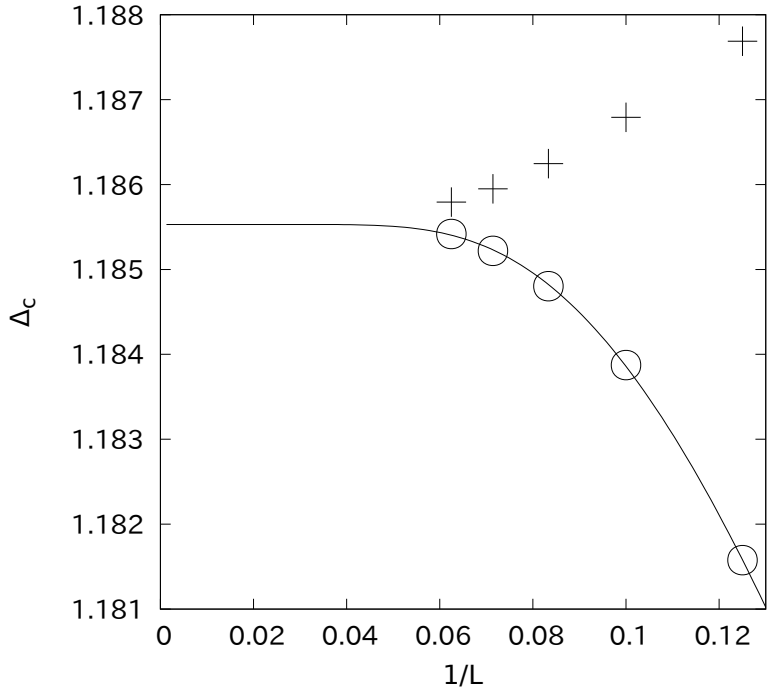

(a)

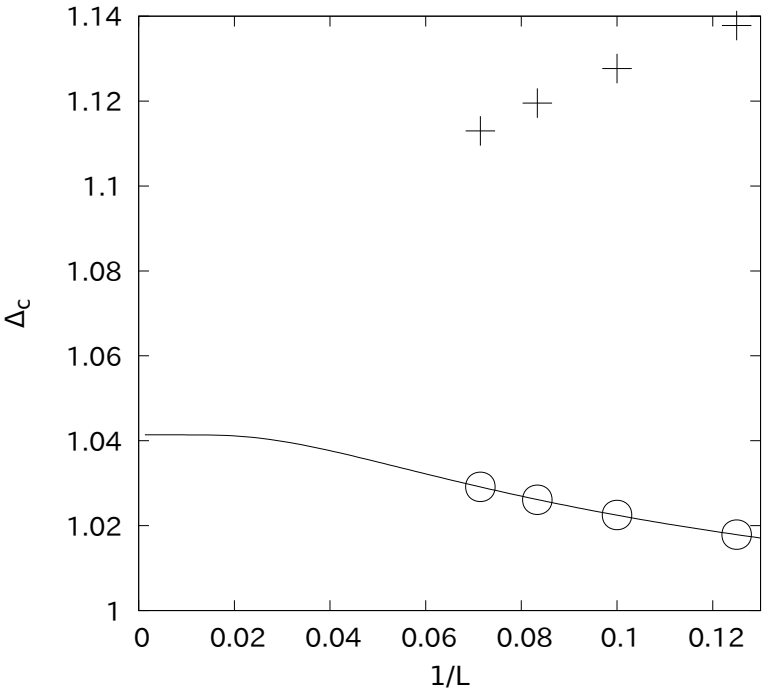

(b)

Figure 4.11: (a),(b): The FSC of a crossing point Δ_c for a S=1 Haldane-Néel transition to a inverse system size $1/N$ respectively for $\delta = 0, 0.25$. Here, we are fixing δ and varying Δ. The $\circ$ and $+$ are the result of the yTBC-zTBC and yTBC-PBC method. Solid line shows the extrapolation.

2D Gaussian universality

The size dependence for Dimer1-Haldane transition is shown in Fig.4.12. Far from AT point, the resulting δ_c using yTBC decrease to system size N and zTBC increase-Fig.4.12(a). But, getting closer At point, the sign of the slope changes Fig.4.12(b). So, we can not proceed the extrapolation.

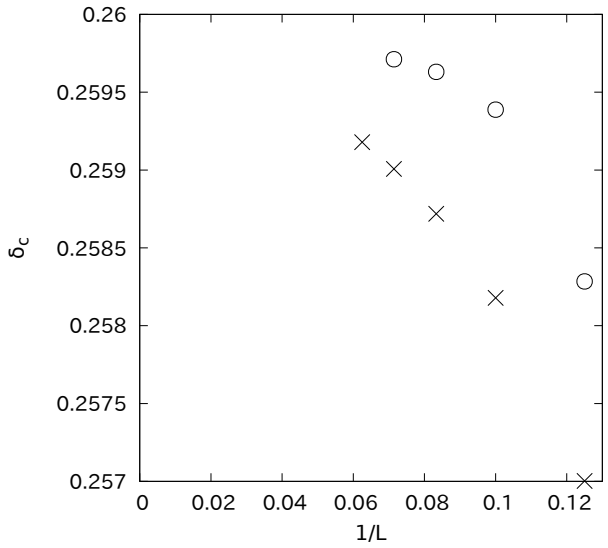

(a)

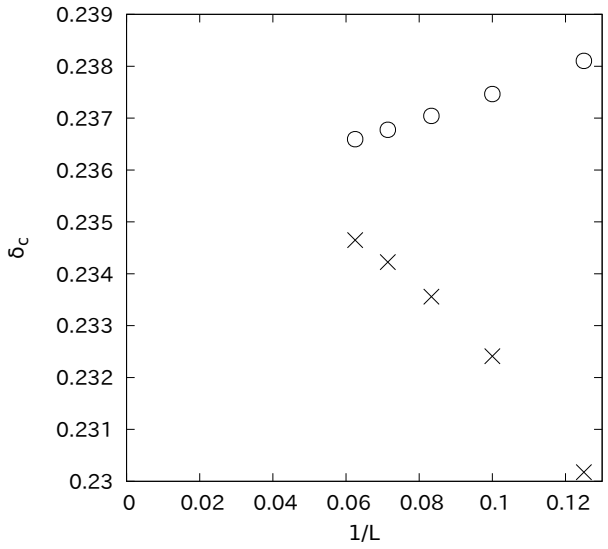

(b)

Figure 4.12: (a),(b): The FSC of a crossing point δ_c for a S=1 dimer1-dimer2 transition to a inverse system size $1/L$ respectively for $\Delta = 0.9, 0.1$. The $\circ$ and $\times$ are the result using yTBC and zTBC respectively.

4.3 $S = 3/2$

For S=3/2, there are more types of the VBS phase, depending on the singlet pairing of divided S=1/2 spins. In a similar way to the case of S=1/2 and 1, we calculate a transition point and can obtain a phase diagram with a small FSC.

4.3.1 Phase Diagram

The S=3/2 spin can be divided to three S=1/2 spins. There are m=$\pm$3/2,$\pm$1/2 VBS phase. The strength of the bond-alternation determine the singlet pair. For the strong bond-alternating case, all the S=1/2 spins take singlet pairing in 2j,2j+1 bond, m=3/2. The bond-alternation become smaller, the one of the singlet pair takes in 2j-1,2j bond, m=1/2. The quantum numbers for each BC are summarized in Table.4.2.

	M=3/2	M=1/2	M=-1/2	M=3/2
PBC	(0,-1)	(0,-1)	(0,-1)	(0,-1)
zTBC	(0,1)	(0,-1)	(0,1)	(0,-1)
yTBC	(even,1)	(odd,-1)	(even,1)	(odd,-1)

Table 4.2: Quantum number (M,P) for $S = 3/2$.

The phase diagram is shown in Fig.4.13(e). The transition line between m=1/2 and m=-1/2 phase is exactly obtained[12], $\delta = 0$.

The phase diagram is shown in Fig.4.13(e).

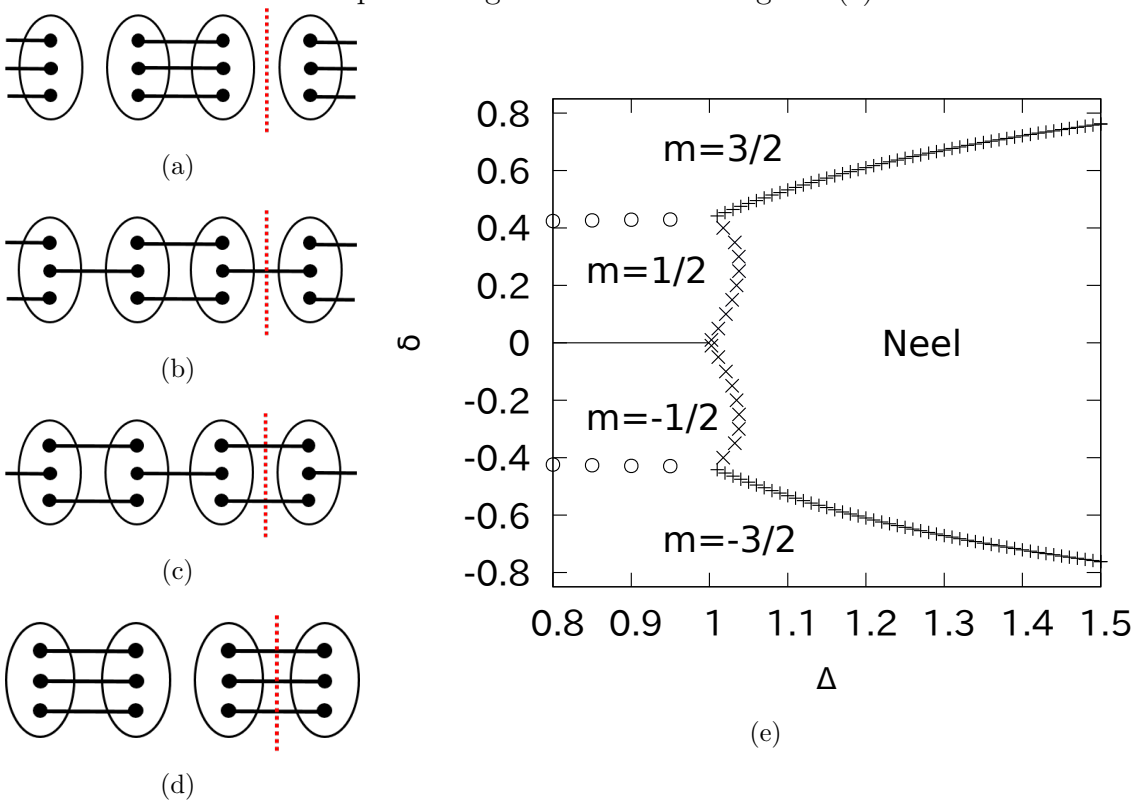

Figure 4.13: (a),(b),(c) : The VBS states taking the different singlet pairing. Dashed lines denote the bond between the N-th and 1st sites. (d) : The phase diagram

2D Ising universality

For S=3/2, we can calculate only for small system size, up to N=12. The size dependence for m=3/2-Néel transition are shown in Fig.4.14. The size dependence for m=3/2-Néel transition are shown in Fig.4.15.

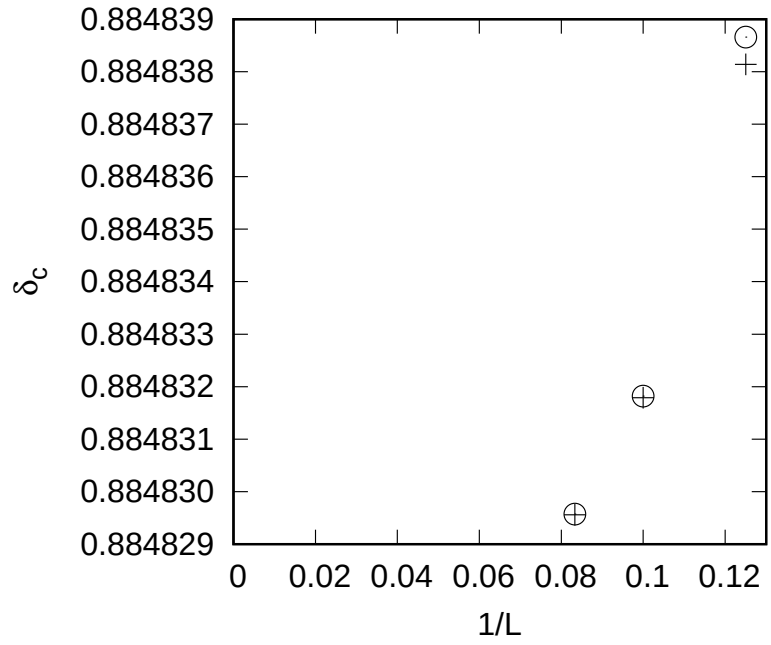

(a)

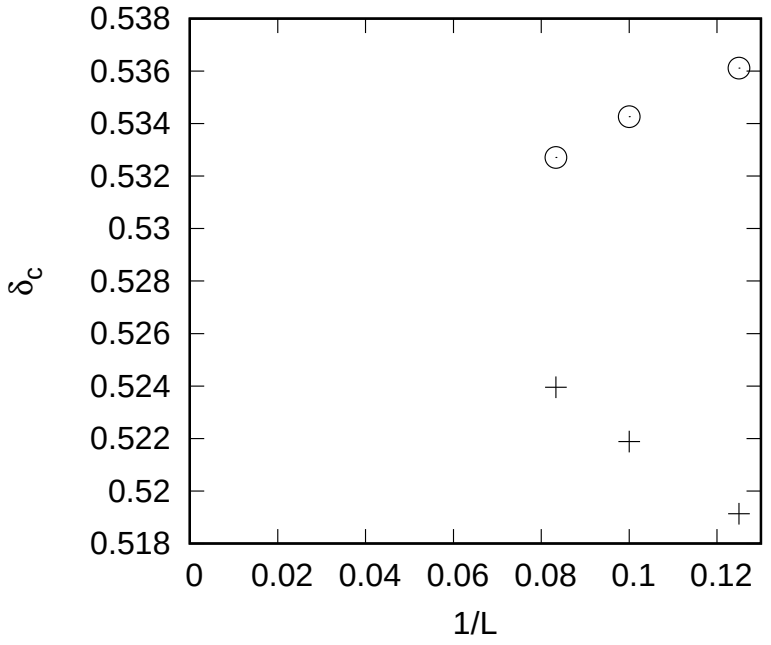

(b)

Figure 4.14: (a),(b): The FSC of a crossing point δ_c for a S=3/2 m=3/2-Néel transition to a inverse system size $1/N$ respectively for $\Delta = 2.0, 1.1$. The $\circ$ and $+$ are the result of the yTBC-zTBC and yTBC-PBC method.

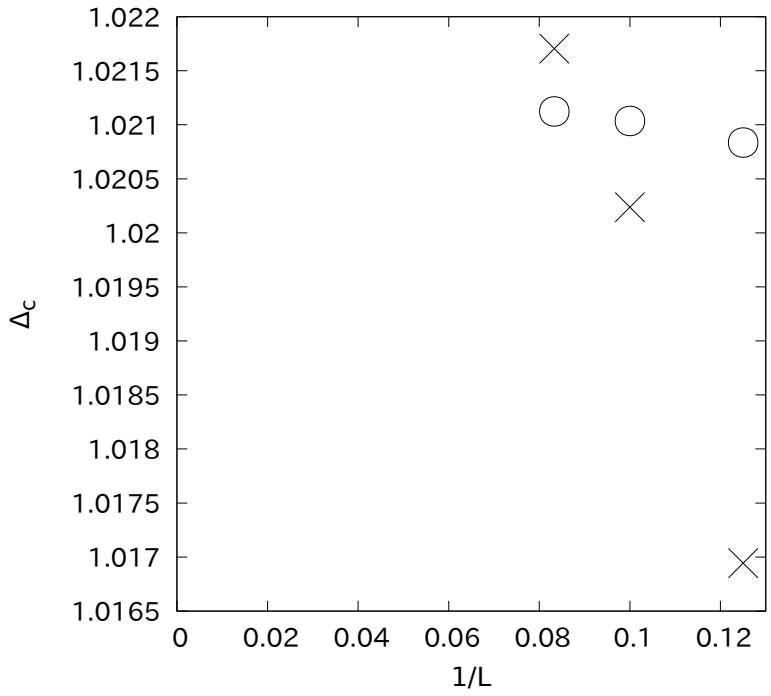

(a)

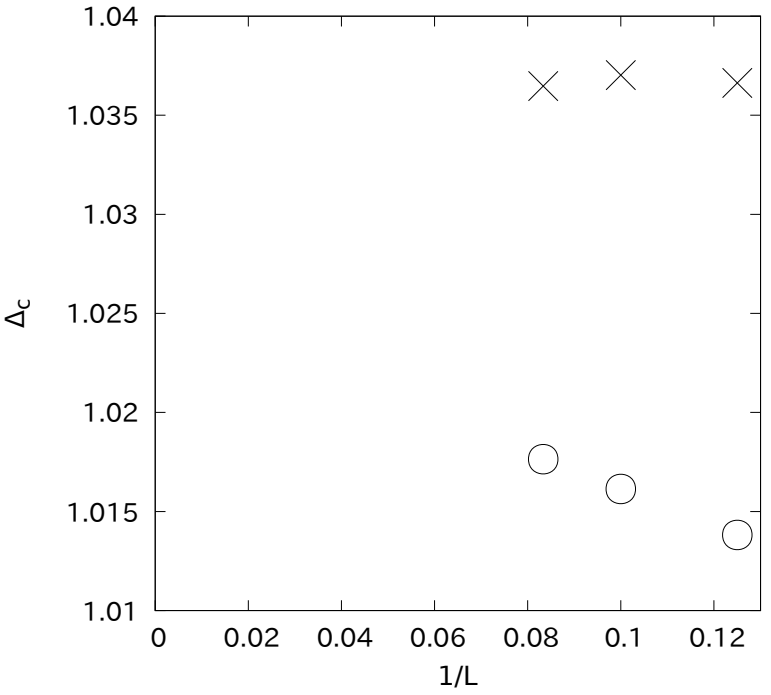

(b)

Figure 4.15: (a),(b): The FSC of a crossing point δ_c for a S=3/2 m=1/2-Néel transition to a inverse system size $1/N$ respectively for $\delta = 0.1, 0.4$. The $\circ$ and $+$ are the result of the yTBC-zTBC and yTBC-PBC method.

2D Gaussian universality

The size dependence for m=3/2-m=1/2 transition is shown in Fig.4.16. The sign of slope changes and we can not proceed the extrapolation. the m=1/2-m=-1/2 transition is exactly calculated to be $\delta = 0$.

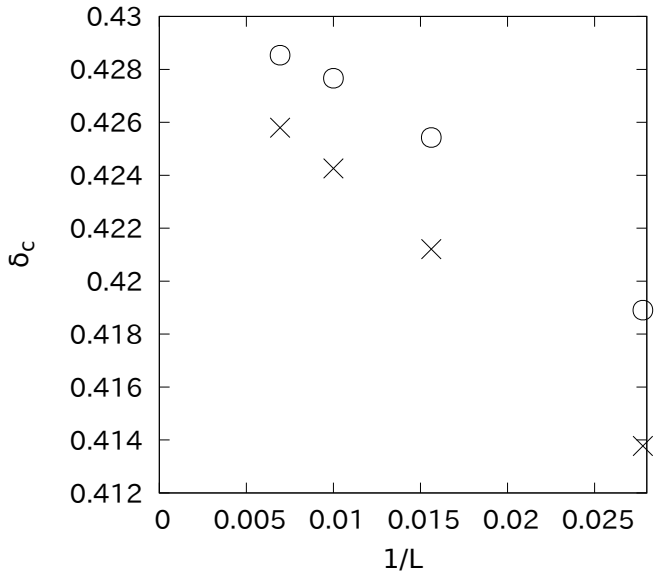

(a)

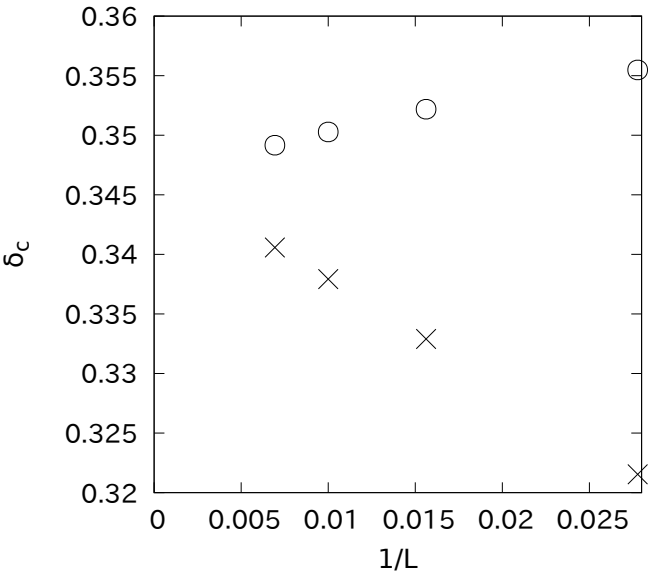

(b)

Figure 4.16: (a),(b): The FSC of a crossing point δ_c for a S=3/2 dimer1-dimer2 transition to a inverse system size $1/N$ respectively for $\Delta = 0.9, 0.1$. The $\circ$ and $\times$ are the results using yTBC and zTBC, respectively.

Chapter 5

Conclusion

We propose a new method to numerically calculate transition points that belong to a 2D Ising universality and a 2D Gaussian universality. We improve the duality transformation of the TFI model, that enable one to treat the boundary conditions and the symmetry of the excited states for a finite system. The energies in periodic and anti-periodic BC cross at the transition point for a finite system. To consider a continuum limit, we discuss a conformal field theory of a free fermion. In the BA XXZ chain, we propose two methods, the yTBC-PBC method (Eq.(2.4.20)) and the yTBC-zTBC method (Eq.(2.4.21)). By anisotropic limit, since the BA XXZ chain is identical to the TFI model, both methods have no FSC. In the AT multicritical point, the yTBC-zTBC method has no FSC, that enables an accurate calculation near the AT multicritical point. We actually calculate the 2D Ising universality transition lines of S=1/2, 1, 3/2 BA XXZ model. As expected, the yTBC-zTBC method has a small FSC near the multicritical point. To confirm the universality class, the central charge and scaling dimensions are calculated. The results are consistent with a 2D Ising model.

Also, we calculate a 2D Gaussian universality transition point using the yTBC. We can distinguish each phase by the parity of magnetization. The numerical results using the yTBC is consistent with the results using the zTBC. The perturbative renormalization calculation for the yTBC is a future task.

We expect that our method can be applied to other quantum spin models.

Acknowledgement

First of all, I thank my supervisor Professor Kiyohide Nomura for many discussions and advices. I thank Professor Jun-ichi Fukuda for giving useful comments and having my manuscript read. I thank Professor Jun Matsui for a valuable advice for coding of the exact diagonalization method. I thank Professor Taku Matsui for a valuable advice. By his advice, I find the proper form of a duality transformation.

My calculation program used in the exact diagonalization is TITPACK Ver.2 coded by H. Nishimori [36]. The modification of the calculation program for yTBC is assisted by a former graduated student Taiju Mukai.

Appendix A

Correspondence to Ashkin-Teller model

A.1 1D Quantum Ashkin-Teller model

The 1D quantum Ashkin-Teller model is composed of the interacting two TFI models

$$\hat{H} = -\beta \sum_{j}^{N} \left(\hat{\sigma}_j^z \hat{\sigma}_{j+1}^z + \hat{\tau}_j^z \hat{\sigma}_{j+1}^z + \lambda \hat{\sigma}_j^z \hat{\sigma}_{j+1}^z \hat{\tau}_j^z \hat{\tau}_{j+1}^z \right) - \sum_{j}^{N} \left(\hat{\sigma}_j^x + \hat{\tau}_j^x + \lambda \hat{\sigma}_j^x \hat{\tau}_j^x \right), \quad \text{(A.1.1)}$$

$\hat{\boldsymbol{\sigma}}_j$ and $\hat{\boldsymbol{\tau}}_j$ are Pauli matrix on different chain. We show correspondence of the BA XXZ model. Dividing the strong bond and weak bond,

$$\begin{aligned} \hat{H} = & \sum_{j}^{N} \left(\hat{S}_{2j-1}^x \hat{S}_{2j}^x + \hat{S}_{2j-1}^y \hat{S}_{2j}^y + \Delta \hat{S}_{2j-1}^z \hat{S}_{2j}^z \right) \\ & + \beta \sum_{N}^{j} \left(\hat{S}_{2j}^x \hat{S}_{2j+1}^x + \hat{S}_{2j}^y \hat{S}_{2j+1}^y + \Delta \hat{S}_{2j}^z \hat{S}_{2j+1}^z \right), \end{aligned} \quad \text{(A.1.2)}$$

$\beta = \frac{1-\delta}{1+\delta}$ and constant factor is ignored. Operating the π rotation operator around the z-axis on even sites, $\hat{G} = \exp\left(i\pi \sum_j^N \hat{S}_{2j}^z \right)$,

$$\begin{aligned} \hat{G}\hat{H}\hat{G}^{-1} = & - \sum_{L}^{j} \left(\hat{S}_{2j-1}^x \hat{S}_{2j}^x + \hat{S}_{2j-1}^y \hat{S}_{2j}^y - \lambda \hat{S}_{2j-1}^z \hat{S}_{2j}^z \right) \\ & - \beta \sum_{L}^{j} \left(\hat{S}_{2j}^x \hat{S}_{2j+1}^x + \hat{S}_{2j}^y \hat{S}_{2j+1}^y - \lambda \hat{S}_{2j}^z \hat{S}_{2j+1}^z . \right) \end{aligned} \quad \text{(A.1.3)}$$

$\frac{\pi}{2}$-rotating all spins around x-axis, $\hat{K} = \exp\left(\frac{-i\pi}{2}\sum_{2L}^{\alpha}\hat{S}_{\alpha}^{x}\right)$,

$$\begin{aligned}\left(\hat{K}\hat{G}\right)\hat{H}\left(\hat{K}\hat{G}\right)^{-1} =& -\sum_{L}^{j}\left(\hat{S}_{2j-1}^{x}\hat{S}_{2j}^{x}+\hat{S}_{2j-1}^{z}\hat{S}_{2j}^{z}-\lambda\hat{S}_{2j-1}^{y}\hat{S}_{2j}^{y}\right)\\ &-\beta\sum_{L}^{j}\left(\hat{S}_{2j}^{x}\hat{S}_{2j+1}^{x}+\hat{S}_{2j}^{z}\hat{S}_{2j+1}^{z}-\lambda\hat{S}_{2j}^{y}\hat{S}_{2j+1}^{y}\right)\end{aligned} \tag{A.1.4}$$

Using $i\hat{S}_{j}^{y} = -\hat{S}_{j}^{x}\hat{S}_{j}^{y}$,

$$\begin{aligned}\left(\hat{K}\hat{G}\right)\hat{H}\left(\hat{K}\hat{G}\right)^{-1} =& -\sum_{L}^{j}\left(\hat{S}_{2j-1}^{x}\hat{S}_{2j}^{x}+\hat{S}_{2j-1}^{z}\hat{S}_{2j}^{z}-\lambda\hat{S}_{2j-1}^{x}\hat{S}_{2j}^{x}\hat{S}_{2j-1}^{z}\hat{S}_{2j}^{z}\right)\\ &-\beta\sum_{L}^{j}\left(\hat{S}_{2j}^{x}\hat{S}_{2j+1}^{x}+\hat{S}_{2j}^{z}\hat{S}_{2j+1}^{z}-\lambda\hat{S}_{2j}^{x}\hat{S}_{2j+1}^{x}\hat{S}_{2j}^{z}\hat{S}_{2j+1}^{z}\right)\end{aligned} \tag{A.1.5}$$

We define the duality transformation

$$\hat{S}_{\alpha}^{x} = \hat{\sigma}_{\alpha-1/2}^{z}\hat{\sigma}_{\alpha+1/2}^{z} \tag{A.1.6}$$

$$\hat{S}_{j}^{z} = \prod_{i=j}^{N}\hat{\sigma}_{i+1/2}^{x} \tag{A.1.7}$$

and

$$\hat{S}_{1}^{x} = \hat{\sigma}_{3/2}^{z}. \tag{A.1.8}$$

The Hamiltonian becomes

$$\begin{aligned}(\hat{K}\hat{G})\hat{H}(\hat{K}\hat{G})^{-1} =& -\beta\sum_{N}^{j=1}\left(\hat{\sigma}_{2j-1/2}^{z}\hat{\sigma}_{2j+3/2}^{z}+\hat{\sigma}_{2j+1/2}^{x}+\lambda\hat{\sigma}_{2j-1/2}^{z}\hat{\sigma}_{2j+1/2}^{z}\hat{\sigma}_{2j+3/2}^{z}\right)\\ &-\sum_{j=1}^{L}\left(\hat{\sigma}_{2j-3/2}^{z}\hat{\sigma}_{2j+1/2}^{z}+\hat{\sigma}_{2j-1/2}^{x}+\lambda\hat{\sigma}_{2j-3/2}^{z}\hat{\sigma}_{2j-1/2}^{z}\hat{\sigma}_{2j+1/2}^{z}\right)\end{aligned} \tag{A.1.9}$$

Replacing the index $j \to \frac{1}{2}\left(j+\frac{1}{2}\right)$ and rewriting the spins on half-odd sites by $\hat{\boldsymbol{\tau}}$

$$\begin{aligned}=& -\beta\sum_{N}^{j=1}\left(\hat{\sigma}_{j}^{z}\hat{\sigma}_{j+1}^{z}+\hat{\tau}_{j+1/2}^{x}+\lambda\hat{\sigma}_{j}^{z}\hat{\tau}_{j+1/2}^{z}\hat{\sigma}_{j+1}^{z}\right)\\ &-\sum_{j=1}^{L}\left(\hat{\tau}_{j-1/2}^{z}\hat{\tau}_{j+1/2}^{z}+\hat{\sigma}_{j}^{x}+\lambda\hat{\tau}_{j-1/2}^{z}\hat{\sigma}_{j}^{z}\hat{\tau}_{j+1/2}^{z}\right)\end{aligned} \tag{A.1.10}$$

Finally, taking the duality transformation only to $\hat{\boldsymbol{\tau}}$, we obtain the 1D Ashkin-Teller model Hamiltonian Eq.(A.1.1).

Appendix B

Field Thoeory of Ising model

B.1 Continuous Limit

Operating π-rotation to the spin around the x-axis

$$\hat{H} = -\sum_{j=0}^{N} \left(\hat{\sigma}_j^x \hat{\sigma}_{j+1}^x - \gamma \hat{\sigma}_j^z \right). \tag{B.1.1}$$

We transform this Hamiltonian to the spin-less Fermion, performing the Jordan-Wigner transformation,

$$\hat{\sigma}_i^+ = \exp\left(i\pi \sum_{j=1}^{i-1} \hat{a}_j^\dagger \hat{a}_j \right) \hat{a}_i^\dagger, \tag{B.1.2}$$

$$\hat{\sigma}_1^+ = -\hat{a}_1^\dagger, \tag{B.1.3}$$

$$\hat{\sigma}_i^z = -1 + 2\hat{a}_i^\dagger \hat{a}_i. \tag{B.1.4}$$

The Hamiltonian is , neglecting the constant term,

$$\hat{H} = -\sum_j \left[\hat{a}_j^\dagger \hat{a}_{j+1} - \hat{a}_j \hat{a}_{j+1}^\dagger + \hat{a}_j^\dagger \hat{a}_{j+1}^\dagger - \hat{a}_j \hat{a}_{j+1} - 2\gamma \hat{a}_j^\dagger \hat{a}_j \right]. \tag{B.1.5}$$

Fourier transformation

$$\hat{a}_j = \frac{1}{\sqrt{N}} \sum_k \exp(iajk) \hat{a}_k. \tag{B.1.6}$$

The Hamiltonian

$$\hat{H} = -\sum_k \left[\left(\exp(ika) \hat{a}_k^\dagger \hat{a}_k - \exp(-ika) \hat{a}_k \hat{a}_k^\dagger + \exp(-ika) \hat{a}_{-k}^\dagger \hat{a}_k^\dagger - \exp(ika) \hat{a}_{-k} \hat{a}_k \right) - 2\gamma \hat{a}_k^\dagger \hat{a}_k \right] \tag{B.1.7}$$

$$= -\sum_k \left(2\left(-\gamma + \cos(ka)\right) \hat{a}_k^\dagger \hat{a}_k + i \sin(ka) \left(\hat{a}_{-k}^\dagger \hat{a}_k^\dagger + \hat{a}_{-k} \hat{a}_k \right) \right) \tag{B.1.8}$$

Taking the continuum limit, the continuum fermion field

$$\Psi(x_j) = \frac{1}{\sqrt{a}}\hat{a}_j, \tag{B.1.9}$$

whose commutation relation is

$$[\Psi(x), \Psi(x')] = \delta(x - x'). \tag{B.1.10}$$

Fourier transformation

$$\hat{a}_k = \int dx \frac{\exp(-ikx)}{\sqrt{Na}}\Psi(x) \tag{B.1.11}$$

$$\Psi(x) = \sum_k \frac{\exp(ikx)}{\sqrt{Na}}\hat{a}_k \tag{B.1.12}$$

In the vicinity of the transition point ($\gamma = 1$), focus on $ka \ll 1$,

$$\hat{H} = 2(\gamma - 1)\int dx \Psi^\dagger(x)\Psi(x) + a\int dx \left(\Psi^\dagger(x)\partial_x\Psi^\dagger(x) - \Psi(x)\partial_x\Psi(x)\right) \tag{B.1.13}$$

In spin-less Fermion operators, the periodic boundary condition ($g = 1$) leads

$$\hat{a}_{N+1} = \hat{a}_1. \tag{B.1.14}$$

The BC of continuum field is

$$\Psi(L) = \Psi(0), \Psi^\dagger(L) = \Psi^\dagger(0). \tag{B.1.15}$$

The anti-periodic boundary condition ($g = -1$) leads

$$\hat{a}_{N+1} = -\hat{a}_1, \tag{B.1.16}$$

$$\Psi(L) = -\Psi(0), \Psi^\dagger(L) = -\Psi^\dagger(0) \tag{B.1.17}$$

Appendix C

Conformal Filed Theory

C.1 Conformal Transformation

We review the conformal field theory. By the infinitesimal transformation ($\epsilon << 1$),

$$r_\mu \to r'_\mu = r_\mu + \epsilon f_\mu(\boldsymbol{r}), \tag{C.1.1}$$

the flat metric,

$$ds^2 = dr_\mu dr_\mu, \tag{C.1.2}$$

transforms to

$$ds'^2 = ds^2 + \epsilon(\partial_\mu f_\nu + \partial_\nu f_\mu) dr_\mu dr_\nu. \tag{C.1.3}$$

The conformal transformation is

$$\partial_\mu f_\nu + \partial_\nu f_\mu = \frac{2}{d}\delta_{\mu\nu}\partial_\lambda f_\lambda, \tag{C.1.4}$$

such f_μ is called *conformal Killing vector*. Eq.(C.1.3) becomes

$$ds'^2 = \left(1 + \epsilon\frac{2}{d}\partial_\lambda f_\lambda\right) ds^2. \tag{C.1.5}$$

The conformal transformation preserve the angle between two vectors, $\boldsymbol{r}\cdot\boldsymbol{r}'/(rr')$. In general, the form of $f(x)$ that satisfy the Eq.(C.1.4) is,

(translation)

$$f_\mu = c_\mu, \tag{C.1.6}$$

(rotation)

$$f_\mu = w_{\mu\nu} r_\nu, w_{\mu\nu} = -w_{\nu\mu}, \tag{C.1.7}$$

(dilatation)

$$f_\mu = a r_\mu, \tag{C.1.8}$$

(special conformal transformation)

$$f_\mu = c_\mu r^2 - 2\boldsymbol{c}\cdot\boldsymbol{r} r_\mu. \tag{C.1.9}$$

We show that the special conformal transformation satisfies Eq.(C.1.4). (The others is easy to calculate.)

$$\begin{aligned}
\partial_\nu f_\mu =& 2c_\mu r_\eta \partial_\nu r_\eta - 2c_\eta r_\mu \partial_\nu r_\eta - 2\boldsymbol{c}\cdot\boldsymbol{r}\partial_\nu r_\mu \\
=& 2c_\mu r_\nu - 2c_\nu r_\mu - 2\boldsymbol{c}\cdot\boldsymbol{r}\delta_{\nu\mu} \\
\partial_\mu f_\nu + \partial_\mu f_\nu =& -4\boldsymbol{c}\cdot\boldsymbol{r}\delta_{\nu\mu} \\
\partial_\mu f_\mu =& 2c_\mu r_\eta \partial_\mu r_\eta - 2c_\eta r_\mu \partial_\mu r_\eta - 2\boldsymbol{c}\cdot\boldsymbol{r}\partial_\mu r_\mu \\
=& -2d\boldsymbol{c}\cdot\boldsymbol{r}
\end{aligned}$$

For $d = 2$, Eq.(C.1.4) becomes Cauchy-Riemann Equation

$$\partial_1\epsilon_1 = \partial_2\epsilon_2 \tag{C.1.10}$$

$$\partial_1\epsilon_2 = -\partial_2\epsilon_1. \tag{C.1.11}$$

Using $z = x_1 + ix_2, \bar{z} = x_1 - ix_2, \epsilon = \epsilon_1 + i\epsilon_2, \bar{\epsilon} = \epsilon_1 - i\epsilon_2$,

$$\partial_{\bar{z}}\epsilon = 0, \partial_z\bar{\epsilon} = 0 \tag{C.1.12}$$

$$ds'^2 = \frac{\partial f}{\partial z}\frac{\partial \bar{f}}{\partial \bar{z}} dz d\bar{z} \tag{C.1.13}$$

The infinitesimal transformations become

$$z' = z + \epsilon_n(z), \bar{z}' = \bar{z} + \bar{\epsilon}_n(\bar{z}), \tag{C.1.14}$$

where

$$\epsilon_n(z) = -z^{n+1}, \bar{\epsilon}_n(\bar{z}) = -\bar{z}^{n+1}. \tag{C.1.15}$$

The generators,

$$l_n = -z^{n+1}\partial_z, \bar{l}_n = -\bar{z}^{n+1}\partial_{\bar{z}}, \tag{C.1.16}$$

construct the Lie algebra,

$$[l_m, l_n] = (m-n)l_{m+n}, \quad [\bar{l}_m, \bar{l}_n] = (m-n)\bar{l}_{m+n}, \quad [l_m, \bar{l}_n] = 0. \tag{C.1.17}$$

C.2 Free Fermion

By taking continuous limit, the critical 2D Ising model is described by free fermion,

$$S = \frac{1}{8\pi}\int dzd\bar{z}\left(\psi\bar{\partial}\psi + \bar{\psi}\partial\bar{\psi}\right) \tag{C.2.1}$$

The short distance singularities are

$$\psi(z)\psi(w) = -\frac{1}{z-w}, \bar{\psi}(\bar{z})\bar{\psi}(\bar{w}) = -\frac{1}{\bar{z}-\bar{w}} \tag{C.2.2}$$

The mode expansion is

$$i\psi(z) = \sum \psi_n z^{-n-1/2}, \tag{C.2.3}$$

n is integers or half-integers, depending on BC. When $n \in \boldsymbol{Z} + \frac{1}{2}$,

$$\psi(e^{2\pi i}z) = +\psi(z). \qquad (P) \tag{C.2.4}$$

When $n \in \boldsymbol{Z}$,

$$\psi(e^{2\pi i}z) = -\psi(z). \qquad (A) \tag{C.2.5}$$

The stress-energy tensor is

$$T(z) = -\frac{1}{2} : \psi(z)\partial\psi(w) : . \tag{C.2.6}$$

The OPE of $T(z)$ and $\psi(z)$ is

$$\begin{aligned}
-\frac{1}{2} : \psi(z)\partial\psi(z) : \psi(w) =& -\frac{1}{2}\langle\psi(z)\psi(w)\rangle\partial\psi(z) + \frac{1}{2}\psi(z)\langle\partial\psi(z)\psi(w)\rangle \\
=& \frac{1}{2}\frac{1}{z-w}\partial\psi(z) + \frac{1}{2}\frac{1}{(z-w)^2}\psi(z) \\
=& \frac{1}{2}\frac{1}{z-w}\left(\partial\psi(w) + \cdots\right) \\
&+ \frac{1}{2}\frac{1}{(z-w)^2}\left(\psi(w) + (z-w)\,\partial\psi(w) + \cdots\right) \\
=& \frac{1}{2}\frac{1}{(z-w)^2}\psi(w) + \frac{1}{z-w}\partial\psi(w) + \cdots .
\end{aligned} \tag{C.2.7}$$

Thus, the primary field $\psi(z)$ has a conformal weight $h = 1/2$. The OPE of the stress-energy tensors is

$$T(z)T(w) = \frac{1/4}{(z-w)^4} + \frac{2}{(z-w)^2}T(w) + \frac{1}{z-w}T(w). \tag{C.2.8}$$

Thus, the central charge is $c = 1/2$.

We calculate the 2-point correlation function in Periodic (P),

$$\begin{aligned}\langle\psi(z)\psi(w)\rangle_P &= -\left\langle \sum_{n=1/2}^{\infty} \psi_n z^{-n-1/2} \sum_{m=1/2}^{\infty} \psi_m w^{-m-1/2} \right\rangle_P \\ &= -\sum_{n=1/2}^{\infty} z^{-n-1/2} w^{-n-1/2} = -\frac{1}{z}\sum_{n=0}^{\infty}\left(\frac{w}{z}\right)^n = \frac{-1}{z-w}. \end{aligned} \tag{C.2.9}$$

For Anti-Periodic case, we introduce the twist operator $\sigma(w)$,

$$\psi(z)\sigma(w) \sim (z-w)^{-1/2}\mu(w) + \cdots \tag{C.2.10}$$

The field μ has the same conformal weight as the field σ.

$$\begin{aligned}\langle\psi(z)\psi(w)\rangle_A &\equiv \langle 0|\, \sigma(\infty)\psi(z)\psi(w)\sigma(0)\,|0\rangle \\ &= -\left\langle \sum_{n=0}^{\infty} \psi_n z^{-n-1/2} \sum_{m=0}^{\infty} \psi_m w^{-m-1/2} \right\rangle_A \\ &= -\sum_{n=1}^{\infty} z^{-n-1/2} w^{-n-1/2} - \frac{1}{2\sqrt{zw}} \\ &= -\frac{1}{\sqrt{zw}}\left(\frac{w}{z-w} + \frac{1}{2}\right) \\ &= -\frac{\sqrt{\frac{z}{w}} + \sqrt{\frac{w}{z}}}{2(z-w)} \end{aligned} \tag{C.2.11}$$

The stress-energy tensor is

$$T(z) = \lim_{z\to w} \frac{1}{2}\left(\psi(z)\partial_w\psi(w) + \frac{1}{(z-w)^2}\right) \tag{C.2.12}$$

From Eq.(C.2.11), $\epsilon = z - w$

$$\begin{aligned}\langle T(z)\rangle_A &= \lim_{z\to w}\frac{1}{2}\left(\langle\psi(z)\partial_w\psi(w)\rangle_A + \frac{1}{(z-w)^2}\right) \\ &= \lim_{z\to w}\frac{1}{2}\left(-\frac{\sqrt{\frac{z}{w}} + \sqrt{\frac{w}{z}}}{2(z-w)^2} + \frac{1}{4w^{3/2}z^{1/2}} + \frac{1}{(z-w)^2}\right) \\ &= \lim_{\epsilon\to 0}\frac{1}{2}\left(-\frac{1}{2}\frac{\left(1+\frac{\epsilon}{w}\right)^{1/2} + \left(1+\frac{\epsilon}{w}\right)^{-1/2}}{\epsilon^2} + \frac{1}{\epsilon^2}\right) + \frac{1}{8}\frac{1}{w^2} \\ &= \lim_{\epsilon\to 0}\frac{1}{2}\left(-\frac{1 + \frac{1}{2}\frac{\epsilon}{w} - \frac{1}{2!\cdot 4}\left(\frac{\epsilon}{w}\right)^2 + \cdots + 1 - \frac{1}{2}\frac{\epsilon}{w} + \frac{3}{2!\cdot 4}\left(\frac{\epsilon}{w}\right)^2 - \cdots}{2\epsilon^2} + \frac{1}{\epsilon^2}\right) + \frac{1}{8}\frac{1}{w^2} \\ &= \frac{1}{16w^2} \end{aligned} \tag{C.2.13}$$

Comparing with the operator product

$$T(w)\sigma(0)\left|0\right\rangle \sim \frac{h_\sigma \sigma(0)}{z^2}\left|0\right\rangle + \cdots , \tag{C.2.14}$$

we find that $h_\sigma = \frac{1}{16}$.

C.3 Free Boson

The action for the free boson field theory is

$$\hat{H} = \int \partial\phi(z,\bar{z})\bar{\partial}\phi(z,\bar{z}). \tag{3.1.1}$$

The OPE of the vertex operator and $\partial\varphi(z)$ is

$$\begin{aligned}
\partial\varphi(z)\mathcal{V}_\alpha(w) =& \sum_{n=0}^{\infty} \frac{(i\alpha)^n}{n!}\partial\varphi(z) : \varphi(w)^n : \\
=& \frac{1}{z-w}\sum_{n=1}^{\infty} \frac{(i\alpha)^n}{(n-1)!} : \varphi(w)^{n-1} : \\
=& -i\alpha\frac{\mathcal{V}_{-\alpha}(w)}{z-w}
\end{aligned} \tag{C.3.1}$$

The OPE of the vertex operator and stress-energy tensor $T(z) =: \partial\varphi(z)\partial\varphi(z) :$ is

$$\begin{aligned}
T(z)\mathcal{V}_{-\alpha}(w) =& \sum_{n=0}^{\infty} \frac{(i\alpha)^n}{n!} : \partial\varphi(z)\partial\varphi(z) :: \varphi(w)^n : \\
=& -\frac{1}{4}\frac{1}{(z-w)^2}\sum_{n=0}^{\infty} \frac{(i\alpha)^n}{(n-2)!} : \varphi(w)^{n-2} : \\
&+ \frac{1}{z-w}\sum_{n=0}^{\infty} \frac{(i\alpha)^n}{n!} : \partial\varphi(z)\varphi(w)^{n-1} : \\
=& \frac{\alpha^2/2}{(z-w)^2}\mathcal{V}_\alpha(w) + \frac{1}{(z-w)}\partial_w\mathcal{V}_\alpha(w).
\end{aligned} \tag{C.3.2}$$

The OPE of the vertex operators is

$$\begin{aligned}
\mathcal{V}_\alpha(z)\mathcal{V}_\beta(w) &= \sum_{n,m}^{\infty} \frac{1}{n!m!} : (\alpha\psi(z))^n :: (\alpha\psi(z))^m : \\
&= \sum_{n,m}^{\infty} \frac{1}{n!m!} (\alpha)^n (\beta)^m \langle\psi(z)\psi(w)\rangle^n \psi(w)^{m-n} \frac{m!}{(m-n)!} \\
&= \sum_{n,l}^{\infty} \frac{1}{n!} (\langle\psi(z)\psi(w)\rangle\alpha\beta)^n (\beta)^l \psi(w)^l \frac{1}{l!} \\
&= \exp(\alpha\beta\langle\psi(z)\psi(w)\rangle) \exp(\beta\psi(w)) \\
&= (z-w)^{-\alpha\beta} \mathcal{V}_\beta(w). \qquad \text{(C.3.3)}
\end{aligned}$$

Appendix D

Anisotropic Limit

D.1 S=1

We derive an effective Hamiltonian for S=1 BA XXZ chain in the anisotropic limit. The non-perturbative Hamiltonian is

$$H_0 = \sum_{j=1}^{N/2} \Delta \hat{S}^z_{2j-1} \hat{S}^z_{2j}, \tag{D.1.1}$$

$$= \sum_{j=1}^{N/2} \hat{h}_j. \tag{D.1.2}$$

The eigenstate and eigenenergies of the two-spin Hamiltonian $\hat{h}_j = \Delta \hat{S}^z_{2j-1} \hat{S}^z_{2j}$ are

$$|1\rangle_{2j-1} |-1_{2j}\rangle, E_0 = -\Delta, \tag{D.1.3}$$

$$|-1\rangle_{2j-1} |1\rangle_{2j}, E_0 = -\Delta, \tag{D.1.4}$$

$$|0\rangle_{2j-1} |0\rangle_{2j}, E_1 = 0, \tag{D.1.5}$$

$$\vdots \tag{D.1.6}$$

The higher excited state are omitted because of no effect to the following calculation. We regard the lowest state as the effective S=1/2 spin state,

$$|\uparrow_j\rangle' = |1\rangle_{2j-1} |-1\rangle_{2j}, \tag{D.1.7}$$

$$|\downarrow_j\rangle' = |-1\rangle_{2j-1} |1\rangle_{2j}. \tag{D.1.8}$$

The perturbative Hamiltonian is

$$\hat{H}' = \sum_j^{N/2} \left(\beta \Delta \hat{S}^z_{2j} \hat{S}^z_{2j+1} \right) + \frac{1}{2} \sum_j^{N/2} \left(\hat{S}^+_{2j-1} \hat{S}^-_{2j} + \hat{S}^-_{2j-1} \hat{S}^+_{2j} \right). \tag{D.1.9}$$

- First-order perturbation
  Similar to the $S = 1/2$ case, the z-direction term operates as

$$\hat{S}^z_{2j}\hat{S}^z_{2j+1}\left|\uparrow_j\uparrow_{j+1}\right\rangle' = -\left|\uparrow_j\uparrow_{j+1}\right\rangle'. \tag{D.1.10}$$

  In the effective space, we get $\hat{S}^z_{2j}\hat{S}^z_{2j+1} \to -4\hat{S'}^z_j\hat{S'}^z_{j+1}$. The x, y-direction have no effect because the lowest state is not generated,

$$\hat{S}^+_{2j-1}\hat{S}^-_{2j}\left|\uparrow\right\rangle'_j = \left|0\right\rangle_{2j-1}\left|0\right\rangle_{2j}. \tag{D.1.11}$$

- Second-order perturbation
  The operators that make the excited state $\left|0\right\rangle\left|0\right\rangle$ are only x,y-direction terms.

$$\hat{S}^+_{2j-1}\hat{S}^-_{2j}\left|\downarrow\right\rangle'_j = 2\left|0\right\rangle_{2j-1}\left|0\right\rangle_{2j}, \tag{D.1.12}$$

$$\hat{S}^-_{2j-1}\hat{S}^+_{2j}\left|\uparrow\right\rangle'_j = 2\left|0\right\rangle_{2j-1}\left|0\right\rangle_{2j}, \tag{D.1.13}$$

  here we use $\hat{S}^{\pm}\left|l,m\right\rangle = \sqrt{l(l+1)-m(m\pm1)}\left|l,m\pm1\right\rangle$. Thus, we obtain four terms that have non-zero matrix element in second order perturbation.

$$\left\langle\downarrow\right|'_j\hat{S}^-_{2j-1}\hat{S}^+_{2j}\left|0\right\rangle_{2j-1}\left|0\right\rangle_{2j}\left\langle0\right|_{2j-1}\left\langle0\right|_{2j}\hat{S}^+_{2j-1}\hat{S}^-_{2j}\left|\downarrow\right\rangle'_j = 4, \tag{D.1.14}$$

$$\left\langle\uparrow\right|'_j\hat{S}^-_{2j-1}\hat{S}^+_{2j}\left|0\right\rangle_{2j-1}\left|0\right\rangle_{2j}\left\langle0\right|_{2j-1}\left\langle0\right|_{2j}\hat{S}^+_{2j-1}\hat{S}^-_{2j}\left|\uparrow\right\rangle'_j = 4. \tag{D.1.15}$$

  These terms are constant terms in the effective space. The other two terms are

$$\left\langle\uparrow\right|'_j\hat{S}^+_{2j-1}\hat{S}^-_{2j}\left|0\right\rangle_{2j-1}\left|0\right\rangle_{2j}\left\langle0\right|_{2j-1}\left\langle0\right|_{2j}\hat{S}^+_{2j-1}\hat{S}^-_{2j}\left|\downarrow\right\rangle'_j = 4, \tag{D.1.16}$$

$$\left\langle\downarrow\right|'_j\hat{S}^-_{2j-1}\hat{S}^+_{2j}\left|0\right\rangle_{2j-1}\left|0\right\rangle_{2j}\left\langle0\right|_{2j-1}\left\langle0\right|_{2j}\hat{S}^-_{2j-1}\hat{S}^+_{2j}\left|\uparrow\right\rangle'_j = 4. \tag{D.1.17}$$

  These terms operate as $4\hat{S'}^+_j$ and $4\hat{S'}^-_j$.

Then, we obtain the effective Hamiltonian

$$\hat{H} = \sum_{j=1}^{N/2}\left(-4\beta\Delta\hat{S'}^z_j\hat{S'}^z_{j+1} + 2\hat{S'}^x_j + 1\right) \tag{D.1.18}$$

D.2 S=3/2

We derive an effective Hamiltonian for S=3/2 BA XXZ chain in the anisotropic limit. The non-perturbative Hamiltonian is

$$H_0 = \sum_{j=1}^{N/2}\Delta\hat{S}^z_{2j-1}\hat{S}^z_{2j}, \tag{D.2.1}$$

$$= \sum_{j=1}^{N/2}\hat{h}_j. \tag{D.2.2}$$

The eigenstate and eigenenergies of the two-spin Hamiltonian $\hat{h}_j = \Delta \hat{S}^z_{2j-1}\hat{S}^z_{2j}$ are

$$|\frac{3}{2}\rangle_{2j-1}|-\frac{3}{2}\rangle_{2j}, E_0 = -\frac{9}{4}\Delta, \tag{D.2.3}$$

$$|-\frac{3}{2}\rangle_{2j-1}|\frac{3}{2}\rangle_{2j}, E_0 = -\frac{9}{4}\Delta, \tag{D.2.4}$$

$$|\frac{1}{2}\rangle_{2j-1}|-\frac{1}{2}\rangle_{2j}, E_1 = -\frac{1}{4}\Delta, \tag{D.2.5}$$

$$|-\frac{1}{2}\rangle_{2j-1}|\frac{1}{2}\rangle_{2j}, E_1 = -\frac{1}{4}\Delta, \tag{D.2.6}$$

$$\vdots \tag{D.2.7}$$

The higher excited state are omitted because of no effect to the following calculation. We regard the lowest state as the effective S=1/2 spin state,

$$|\uparrow_j\rangle' = |\frac{3}{2}\rangle_{2j-1}|-\frac{3}{2}\rangle_{2j}, \tag{D.2.8}$$

$$|\downarrow_j\rangle' = |-\frac{3}{2}\rangle_{2j-1}|\frac{3}{2}\rangle_{2j}. \tag{D.2.9}$$

The perturbative Hamiltonian is

$$\hat{H}' = \sum_j^{N/2}\left(\beta\Delta\hat{S}^z_{2j}\hat{S}^z_{2j+1}\right) + \frac{1}{2}\sum_j^{N/2}\left(\hat{S}^+_{2j-1}\hat{S}^-_{2j} + \hat{S}^-_{2j-1}\hat{S}^+_{2j}\right). \tag{D.2.10}$$

- First-order perturbation
  Similar to the $S = \frac{1}{2}$ case, the z-direction term operates as

  $$\hat{S}^z_{2j}\hat{S}^z_{2j+1}|\uparrow_j\uparrow_{j+1}\rangle' = -\frac{9}{4}|\uparrow_j\uparrow_{j+1}\rangle'. \tag{D.2.11}$$

  In the effective space, we get $\hat{S}^z_{2j}\hat{S}^z_{2j+1} \to -9\hat{S'}^z_j\hat{S'}^z_{j+1}$. Same as the S=1 case, the x, y-direction have no effect because the lowest state is not generated.

- Second-order perturbation
  Only constant term remains.

  $$\langle\downarrow|'_j\,\hat{S}^-_{2j-1}\hat{S}^+_{2j}|-\frac{1}{2}\rangle_{2j-1}|\frac{1}{2}\rangle_{2j}\langle-\frac{1}{2}|_{2j-1}\langle\frac{1}{2}|_{2j}\,\hat{S}^+_{2j-1}\hat{S}^-_{2j}|\downarrow\rangle'_j = 9, \tag{D.2.12}$$

  $$\langle\uparrow|'_j\,\hat{S}^+_{2j-1}\hat{S}^-_{2j}|-\frac{1}{2}\rangle_{2j-1}|\frac{1}{2}\rangle_{2j}\langle-\frac{1}{2}|_{2j-1}\langle\frac{1}{2}|_{2j}\,\hat{S}^-_{2j-1}\hat{S}^+_{2j}|\uparrow\rangle'_j = 9. \tag{D.2.13}$$

- Third-order perturbation

  $$\langle\downarrow|'_j\,\hat{S}^-_{2j-1}\hat{S}^+_{2j}|-\frac{1}{2}\rangle_{2j-1}|\frac{1}{2}\rangle_{2j}\langle-\frac{1}{2}|_{2j-1}\langle\frac{1}{2}|_{2j}\,\hat{S}^-_{2j-1}\hat{S}^+_{2j}|\frac{1}{2}\rangle_{2j-1}|-\frac{1}{2}\rangle_{2j}\langle\frac{1}{2}|_{2j-1}\langle-\frac{1}{2}|_{2j}\,\hat{S}^-_{2j-1}\hat{S}^+_{2j}|\uparrow\rangle'_j$$
  $$=36 \tag{D.2.14}$$

  These terms operate as $36\hat{S}^+_j$ and $36\hat{S}^-_j$.

Then, we obtain the effective Hamiltonian

$$\hat{H} = \sum_{j=1}^{N/2} \left(-9\beta\Delta \hat{S}_j^z \hat{S}_{j+1}^z + \frac{9}{2} \hat{S}_j^x + 9 \right) \tag{D.2.15}$$

Appendix E

Bosonization

E.1 XXZ chain

We review the bosonization method [21] [22] for the XXZ chain

$$\hat{H}_0 = J\sum_i^N \left[\frac{1}{2}\left(\hat{S}_i^+\hat{S}_{i+1}^- + \hat{S}_i^-\hat{S}_{i+1}^+\right) + \Delta\hat{S}_i^z\hat{S}_{i+1}^z\right] \tag{E.1.1}$$

The spin operators obey the mixed set of commutation relation,

$$\left[\hat{S}_i^+, \hat{S}_i^-\right] \tag{E.1.2}$$

When imposing zTBC, the boundary term becomes

$$-\frac{1}{2}\left(\hat{S}_i^+\hat{S}_{i+1}^- + \hat{S}_i^-\hat{S}_{i+1}^+\right) + \Delta\hat{S}_i^z\hat{S}_{i+1}^z \tag{E.1.3}$$

When yTBC,

$$-\frac{1}{2}\left(\hat{S}_i^+\hat{S}_{i+1}^+ + \hat{S}_i^-\hat{S}_{i+1}^-\right) - \Delta\hat{S}_i^z\hat{S}_{i+1}^z \tag{E.1.4}$$

We perform the Jordan-Wigner transformation,

$$\hat{S}_i^+ = \exp\left(-i\pi\sum_{j=1}^{i-1}\hat{a}_j^\dagger\hat{a}_j\right)\hat{a}_i^\dagger, \tag{E.1.5}$$

$$\hat{S}_1^+ = -\hat{a}_1^\dagger, \tag{E.1.6}$$

$$\hat{S}_i^z = -\frac{1}{2} + \hat{a}_i^\dagger\hat{a}_i, \tag{E.1.7}$$

$$\hat{S}_i^+\hat{S}_{i+1}^- = \hat{a}_i^\dagger\hat{a}_{i+1}, \tag{E.1.8}$$

$$\hat{S}_i^-\hat{S}_{i+1}^+ = -\hat{a}_i\hat{a}_{i+1}^\dagger, \tag{E.1.9}$$

$$\hat{S}_i^+\hat{S}_{i+1}^+ = \hat{a}_i^\dagger\hat{a}_{i+1}^\dagger, \tag{E.1.10}$$

$$\hat{S}_i^-\hat{S}_{i+1}^- = -\hat{a}_i\hat{a}_{i+1}. \tag{E.1.11}$$

The commutators of fermionic operator are

$$\left\{\hat{a}_k^\dagger, \hat{a}_{k'}^\dagger\right\} = \{\hat{a}_k, \hat{a}_{k'}\} = 0 \tag{E.1.12}$$

$$\left\{\hat{a}_k^\dagger, \hat{a}_{k'}\right\} = \delta_{kk'} \tag{E.1.13}$$

$$\left[\hat{a}_k^\dagger, \hat{a}_{k'}\right] = 2\hat{a}_k^\dagger \hat{a}_{k'} - \delta_{kk'}. \tag{E.1.14}$$

We define the total number operator

$$\hat{\mathcal{M}} = \sum_j^N \hat{a}_j^\dagger \hat{a}_j \tag{E.1.15}$$

In boundary,

$$\hat{S}_N^+ \hat{S}_1^- = -\exp\left(-i\pi \sum_j^{N-1} \hat{a}_j^\dagger \hat{a}_j\right) \hat{a}_N^\dagger \hat{a}_1 \tag{E.1.16}$$

$$= -(-1)^{\hat{\mathcal{M}}}\, \hat{a}_N^\dagger \hat{a}_1 \tag{E.1.17}$$

$$\hat{S}_N^- \hat{S}_1^+ = (-1)^{\hat{\mathcal{M}}}\, \hat{a}_N \hat{a}_1^\dagger \tag{E.1.18}$$

$$\hat{S}_N^+ \hat{S}_1^+ = -(-1)^{\hat{\mathcal{M}}}\, \hat{a}_N^\dagger \hat{a}_1^\dagger \tag{E.1.19}$$

$$\hat{S}_N^- \hat{S}_1^- = (-1)^{\hat{\mathcal{M}}}\, \hat{a}_N \hat{a}_1 \tag{E.1.20}$$

The Hamiltonian becomes

$$\hat{H} = \frac{J}{2} \sum_i^{N-1} \left(\hat{a}_i^\dagger \hat{a}_{i+1} - \hat{a}_i \hat{a}_{i+1}^\dagger\right) + J\Delta \sum_i^{N-1} \left(-\frac{1}{2} + \hat{a}_i^\dagger \hat{a}_i\right)\left(-\frac{1}{2} + \hat{a}_{i+1}^\dagger \hat{a}_{i+1}\right) + (\text{boundary term}). \tag{E.1.21}$$

In PBC, boundary term is

$$\frac{J}{2}(-1)^{\hat{\mathcal{M}}}\left(-\hat{a}_N^\dagger \hat{a}_1 + \hat{a}_N \hat{a}_1^\dagger\right) + J\Delta\left(-\frac{1}{2} + \hat{a}_N^\dagger \hat{a}_N\right)\left(-\frac{1}{2} + \hat{a}_1^\dagger \hat{a}_1\right) \tag{E.1.22}$$

When the number of fermion is even, the fermion operator obey the anti-periodic boundary condition

$$\hat{a}_{N+1} = -\hat{a}_1, \hat{a}_{N+1}^\dagger = -\hat{a}_1^\dagger \tag{E.1.23}$$

When the number of fermion is odd, the fermion operator obey the periodic boundary condition

$$\hat{a}_{N+1} = \hat{a}_1, \hat{a}_{N+1}^\dagger = \hat{a}_1^\dagger \tag{E.1.24}$$

Because of the translational invariance, we perform the Fourier transformation

$$\hat{a}_j = \frac{1}{\sqrt{N}} \sum_k \exp(ijk)\hat{a}_k. \tag{E.1.25}$$

When fermion number is even,

$$\hat{a}_{N+1} = -\hat{a}_1 \tag{E.1.26}$$

$$k = \frac{\pi(2n-1)}{N} \qquad (-\frac{N}{2}+1 \geq n \geq \frac{N}{2}) \tag{E.1.27}$$

When fermion particle number is odd,

$$\hat{a}_{N+1} = \hat{a}_1 \tag{E.1.28}$$

$$k = \frac{2\pi n}{N} \qquad (-\frac{N}{2}+1 \geq n \geq \frac{N}{2}) \tag{E.1.29}$$

a is the lattice spacing.

$$\sum_j \hat{a}_j^\dagger \hat{a}_{j+1} = \frac{1}{N} \sum_j \sum_{k,k'} \exp(iaj(-k+k') + iak')\hat{a}_k^\dagger \hat{a}_{k'} \tag{E.1.30}$$

$$= \sum_k \exp(iak)\hat{a}_k^\dagger \hat{a}_k \tag{E.1.31}$$

$$\hat{a}_N \hat{a}_1 = \frac{1}{N} \sum_{kk'} \left(-(-1)^{\hat{\mathcal{M}}}\right) \exp(iak')\hat{a}_k \hat{a}_{k'} \tag{E.1.32}$$

$$\hat{a}_N^\dagger \hat{a}_1^\dagger = \frac{1}{N} \sum_{kk'} \left(-(-1)^{\hat{\mathcal{M}}}\right) \exp(-iak')\hat{a}_k^\dagger \hat{a}_{k'}^\dagger \tag{E.1.33}$$

The z-direction term is

$$\sum_j \hat{a}_j^\dagger \hat{a}_j = \sum_k \hat{a}_k^\dagger \hat{a}_k \tag{E.1.34}$$

$$\sum_j \hat{a}_j^\dagger \hat{a}_j \hat{a}_{j+1}^\dagger \hat{a}_{j+1} = \frac{1}{N^2} \sum_j \sum_{k_1,k_2,k_3,k_4} \hat{a}_{k_1}^\dagger \hat{a}_{k_2} \hat{a}_{k_3}^\dagger \hat{a}_{k_4} \exp(ij(-k_1+k_2-k_3+k_4) + i(-k_3+k_4)). \tag{E.1.35}$$

The non-vanishing terms are $-k_1+k_2-k_3+k_4 = 2\pi n$ $(n = 0, \pm 1)$. Rename the wave number as $k = k_2, k' = k_4, q = -k_3 + k_4 - \pi n$

$$= \frac{1}{N} \sum_{kk'q} \cos(q)\hat{a}_{k+q}^\dagger \hat{a}_{k'-q}^\dagger \hat{a}_{k'} \hat{a}_k - \frac{1}{N} \sum_{kk'q} \cos(q)\hat{a}_{k+q\pm\pi}^\dagger \hat{a}_{k'-q\pm\pi}^\dagger \hat{a}_{k'} \hat{a}_k, \tag{E.1.36}$$

q is taken in $\frac{\pi}{N} \geq q \geq \pi - \frac{\pi}{N}$ when number is even or $\frac{2\pi}{N} \geq q \geq \pi$ when number is odd. The XY terms are

$$\sum_j \left(\hat{a}_j^\dagger \hat{a}_{j+1} - \hat{a}_j \hat{a}_{j+1}^\dagger\right) = \sum_k \left(\exp\left(ik\right) + \exp\left(-ik\right)\right) \hat{a}_k^\dagger \hat{a}_k \tag{E.1.37}$$

$$= \sum_k 2\cos\left(k\right) \hat{a}_k^\dagger \hat{a}_k \tag{E.1.38}$$

$$\frac{1}{N} \sum_j \exp\left(ij\left(k - k'\right)\right) = \delta_{kk'} \tag{E.1.39}$$

$$\epsilon(k) = J\left(\cos k - \Delta\right) \tag{E.1.40}$$

$$V(q) = J\Delta \cos q \tag{E.1.41}$$

The Hamiltonian becomes

$$\hat{H} = \sum_k \epsilon(k) \hat{a}_k^\dagger \hat{a}_k + \frac{1}{N} \sum_{kk'q} V(q) \hat{a}_{k+q}^\dagger \hat{a}_{k'-q}^\dagger \hat{a}_{k'} \hat{a}_k - \frac{1}{N} \sum_{kk'q} V(q) \hat{a}_{k+q\pm G/2}^\dagger \hat{a}_{k'-q\pm G/2}^\dagger \hat{a}_{k'} \hat{a}_k. \tag{E.1.42}$$

When $\Delta = 0$, the ground state is occupied in $-\frac{\pi}{2} < k < \frac{\pi}{2}$. Only considering the low-lying excited states, we introduce $\hat{a}_{1,k}$ ($\hat{a}_{2,k}$) operators that have positive (negative) group velocity.

$$\hat{a}_j = \exp\left(i\frac{\pi}{2}j\right) \hat{a}_{1,j} = \exp\left(-i\frac{\pi}{2}j\right) \hat{a}_{2,j} \tag{E.1.43}$$

Using boson density operators

$$\rho_1(k) = \sum_p \hat{a}_{1,p+k}^\dagger \hat{a}_{1,p} \tag{E.1.44}$$

$$\rho_2(k) = \sum_p \hat{a}_{2,p+k}^\dagger \hat{a}_{2,p}, \tag{E.1.45}$$

the Hamiltonian is

$$\begin{aligned} \hat{H}_0 =& \frac{2\pi J}{N} \sum_{q>0} \left(\hat{\rho}_1(q)\hat{\rho}_2(-q) + \hat{\rho}_2(q)\hat{\rho}_2(-q)\right) \\ &+ \frac{J\Delta}{N} \sum_q \left(\hat{\rho}_1(q)\hat{\rho}_1(-q) + \hat{\rho}_2(q)\hat{\rho}_2(-q) + 4\hat{\rho}_1(q)\hat{\rho}_2(-q)\right) \end{aligned} \tag{E.1.46}$$

The commutation relation of boson density operators is

$$[\rho_1(-p), \rho_1(p')] = [\rho_2(-p), \rho_2(p')] = \frac{pL}{2\pi} \delta_{p,p'}. \tag{E.1.47}$$

This can be checked by the evaluation of the vacuum expectation value [37]

$$\langle 0|\left[\rho_1(-p),\rho_1(p)\right]|0\rangle = \frac{pL}{2\pi} \tag{E.1.48}$$

Using the following variables

$$\theta_\pm(x) = i\sum_{q\neq 0}\left(\rho_1(q)\pm\rho_2(q)\right)A_q(x), \tag{E.1.49}$$

$$A_q(x) = \frac{2\pi}{Lq}\exp\left(-\frac{\alpha}{2}|q| - iqx\right), \tag{E.1.50}$$

$$\theta(x) = \theta_+(x), \tag{E.1.51}$$

$$p(x) = -\frac{1}{4\pi}\nabla\theta_-(x), \tag{E.1.52}$$

we obtain the phase Hamiltonian

$$\hat{H} = \int dx\left[A\left(\nabla\theta\right)^2 + Cp^2 - B\cos\theta + D\cos 2\theta\right], \tag{E.1.53}$$

where p is the momentum density conjugate to θ

$$\left[\theta\left(x\right), p\left(x'\right)\right] = i\delta\left(x-x'\right) \tag{E.1.54}$$

The constants A, B, C and D are

$$A = \frac{Ja}{8\pi}\left(1+\frac{3\Delta}{\pi}\right), C = 2\pi Ja\left(1-\frac{\Delta}{\pi}\right), \tag{E.1.55}$$

$$B = \frac{J\delta}{a}, D = \frac{\pi^2\Delta J}{8a}. \tag{E.1.56}$$

E.2 Boundary Condition

In this section, we consider the BC of the phase field θ. The spin operators $\hat{\boldsymbol{S}}$ are related to fermion field operators ψ as

$$\hat{S}^-(x) = (2s)^{-1/2}\left[\psi_1(x)+\psi_2(x)\right]\exp\left(-\hat{N}(x)\right), \tag{E.2.1}$$

$$\hat{S}^+(x) = \left[\hat{S}^-(x)\right]^\dagger, \tag{E.2.2}$$

$$= (2s)^{-1/2}\left[\psi_1^\dagger(x)+\psi_2^\dagger(x)\right]\exp\left(-\hat{N}(x)\right), \tag{E.2.3}$$

$$\hat{S}^z(x) = \hat{\rho}_1(x)+\hat{\rho}_2(x)+\psi_1^\dagger(x)\psi_2(x)+\psi_2^\dagger(x)\psi_1(x). \tag{E.2.4}$$

N is defined as

$$\hat{N}(x) = i\pi \int_0^{x-s/2} dy \left[\hat{\rho}_1(y) + \hat{\rho}_2(y)\right], \tag{E.2.5}$$

$$\hat{\rho}_1(x) = (N)^{\frac{3}{2}}\, \hat{a}^\dagger_{1,j}\hat{a}_{1,j}. \tag{E.2.6}$$

The phase field θ is related to the fermion operators as

$$\psi_1(x) = \frac{1}{\sqrt{2\pi\alpha}} \exp\left[ik_F x - \frac{1}{2i}\left(\theta_+(x) + \theta_-(x)\right)\right] \tag{E.2.7}$$

$$\psi_2(x) = \frac{1}{\sqrt{2\pi\alpha}} \exp\left[-ik_F x + \frac{1}{2i}\left(\theta_+(x) - \theta_-(x)\right)\right] \tag{E.2.8}$$

In continuum limit, spin operators in the zTBC become

$$\hat{S}^+(L) = -\hat{S}^+(0), \hat{S}^-(L) = -\hat{S}^-(0), \hat{S}^z(L) = \hat{S}^z(0). \tag{E.2.9}$$

From the above relations, the zTBC of fermion field operators is

$$\psi_1(L) = -\psi_1(0), \psi_1^\dagger(L) = -\psi_1^\dagger(0) \tag{E.2.10}$$

$$\psi_2(L) = -\psi_2(0), \psi_2^\dagger(L) = -\psi_2^\dagger(0) \tag{E.2.11}$$

Then, the boundary condition of phase field in the zTBC is

$$\theta_+(L) = \theta_+(0) + 2\pi \tag{E.2.12}$$

$$\theta_-(L) = \theta_-(0) \tag{E.2.13}$$

The yTBC in continuum spin operators

$$\hat{S}^+(L) = -\hat{S}^-(0), \hat{S}^-(L) = -\hat{S}^+(0), \hat{S}^z(L) = -\hat{S}^z(0) \tag{E.2.14}$$

correspond to the following BC of fermion field operators

$$\begin{array}{l} \psi_1(L) = -\psi_1^\dagger(0), \psi_1^\dagger(L) = -\psi_1(0) \\ \psi_2(L) = -\psi_2^\dagger(0), \psi_2^\dagger(L) = -\psi_2(0) \end{array}. \tag{E.2.15}$$

The boundary condition of the phase field in yTBC is

$$\theta_+(L) = -\theta_+(0) + 2\pi \tag{E.2.16}$$

$$\theta_-(L) = -\theta_-(0). \tag{E.2.17}$$

Appendix F

Lanczos Method

F.1 Tridiagozalization

The Lanczos method is the tridiagonalization method of the hermitian Hamiltonian $\hat{H}$. The eigenvalue of the tridiagonalized matrix $\mathbf{B}$ can be calculated by bisection method.

The Hamiltonian can be tridiagonalized by unitary matrix $\mathbf{P}$,

$$\mathbf{B} = \mathbf{P}^{-1}\hat{H}\mathbf{P}, \tag{F.1.1}$$

$$= \begin{pmatrix} \alpha_1 & \beta_1 & & & 0 & \\ \beta_1 & \alpha_2 & \beta_2 & & & \\ & \beta_2 & \alpha_3 & \beta_3 & & \\ & & \ddots & \ddots & \ddots & \\ & & & \beta_{n-2} & \alpha_{n-1} & \beta_{n-1} \\ & 0 & & & \beta_{n-1} & \alpha_n \end{pmatrix} \tag{F.1.2}$$

We define the j-th column of $\mathbf{P}$ as the vector u_j,

$$\mathbf{P} = [u_1, u_2, \cdots, u_n] \tag{F.1.3}$$

From the orthogonality of $\mathbf{P}$,

$$u_i^T u_j = \delta_{i,j} \tag{F.1.4}$$

From $\hat{H}\mathbf{P} = \mathbf{PB}$,

$$\begin{aligned} \hat{H}u_1 &= \alpha_1 u_1 + \beta_1 u_2, \\ \hat{H}u_2 &= \beta_1 u_1 + \alpha_2 u_2 + \beta_2 u_3, \\ &\cdots \\ \hat{H}u_k &= \beta_{k-1} u_{k-1} + \alpha_k u_k + \beta_k u_{k+1}, \\ &\cdots \\ \hat{H}u_n &= \beta_{n-1} u_{n-1} + \alpha_n u_n. \end{aligned} \tag{F.1.5}$$

Multiplying u_k^T,

$$\alpha_k = u_k^T \hat{H} u_k. \tag{F.1.6}$$

$$v_{k+1} \equiv \beta_k u_{k+1} = \hat{H} u_k - \beta_{k-1} u_{k-1} - \alpha_k u_k \tag{F.1.7}$$

Bibliography

[1] H.Nishimori, K.Okamoto and M. Yokozawa, J. Phys. Soc. Jpn, 56, 4126 (1987).

[2] Tzeng YC, Dai L, Chung MC, Amico L, Kwek LC. Sci Rep 6, 26453 (2016).

[3] J. Ashkin and E. Teller, Phys. Rev. 64, 178 (1943).

[4] C. Fan, Phys. Lett. A 39, 136 (1972).

[5] M.Kohmoto, M. den Nijs, and L. P. Kadanoff, Phys. Rev. B 24, 5229 (1981).

[6] H. A. Bethe, Zur theorie der metalle. Zeit. f ¨ ur Physik 71 (1931) 205–226

[7] L.P.Kadanoff, Phys. Rev. B22, 1405, (1980).

[8] A. Kitazawa, J. Phys. A30, L285 (1997).

[9] F.D.M. Haldane. Phys. Rev. Lett, 50, 1153, (1983).

[10] K. Nomura and A. Kitazawa, J. Phys. A.: Math. Gen. 31, 7341 (1998).

[11] K.Nomura and A.Kitazawa, J. Phys. Soc. Jpn 66, 12, (1997).

[12] A. Kitazawa and K. Nomura, J. Phys. Soc. Jpn 66, 11, (1997).

[13] L.Onsager, Phys.Rev, 65,117 (1944).

[14] P.Pfeuty, Ann. of Phys, 57,79 (1970).

[15] E.H.Lieb, T.D.Schultz, and D.C.Mattis, Ann. Phys. (N.Y.), 16,407 (1961).

[16] H. A. Kramers and G. H. Wannier, Phys. Rev. 60, 252 (1941).

[17] J. B. Kogut,Rev.Mod.Phys.51659 (1979).

[18] D. E. Evans, J. T. Lewis Comm. Math. Phys. 102(4): 521-535 (1986).

[19] G.Cabrera and R.Jullien. Phys. Rev. B35, 7062 (1987).

[20] M.Yamanaka, Y.Hatsugai, and M.Kohmoto. Phys. Rev. B48, 9555, (1993).

[21] T. Nakano and H. Fukuyama, J. Phys. Soc. Jpn. 50, 2489 (1981)

[22] T.Nakano and H.Fukuyama: J. Phys. Soc. Jpn. 50 (1981) 2489.

[23] H. W. J.Blöte, J. L.Cardy and M. P.Nightingale:Phys. Rev. Lett. 56 (1986) 742.

[24] J.L.Cardy, Nucl. Phys. B270, 186 (1986).

[25] C. Lanczos, J. Res. Nat. Bureau of Standards 45, 255-282 (1950).

[26] M. P.Nightingale and H. W.Blöte, Phys. Rev. B 33 659 (1986).

[27] S. R.White and D. A.Huse, Phys. Rev. B 48 3844 (1993).

[28] I. Affleck, E. H. Lieb,Lett Math Phys 12, 57–69 (1986).

[29] D. Guo. T. Kennedy, S. Mazumdar, Phys. Rev. B41 9592 (1990).

[30] M. Oshikawa, J. Phys. Condens. Matter 4, 7469 (1992).

[31] A. Kitazawa and K. Nomura: J. Phys. Soc. Jpn. 66 (1997) 3379

[32] Ejima Satoshi and Fehske Holger PhysRevB.91.045121 2015.

[33] G.Gómez-Santos: Phys. Rev. Lett. 63 (1989) 790.

[34] K.Nomura:Phys. Rev. B 40 (1989) 9142.

[35] T.Sakai and M.Takahashi: J. Phys. Soc. Jpn. 59 (1990) 2688.

[36] H.Nishimori and Y.Taguchi. Prog. Theor. Phys. Suppl, 87 247 (1986).

[37] D. C.Mattis and E. H.Lieb: J. Math. Phys. 6 (1965) 304.